Accepted Manuscript

Design, synthesis, and discovery of ocotillol-type amide derivatives as orally available modulators of *P*-glycoprotein-mediated multidrug resistance

Qianwen Ren, Gangqiang Yang, Mengqi Guo, Jingwen Guo, Yang Li, Jing Lu, Qing Yang, Hanhan Tang, Yi Li, Xiaojuan Fang, Yixiao Sun, Jia Grace Qi, Jingwei Tian, Hongbo Wang

PII: S0223-5234(18)30907-3

DOI: 10.1016/j.ejmech.2018.10.038

Reference: EJMECH 10824

To appear in: *European Journal of Medicinal Chemistry*

Received Date: 14 August 2018

Revised Date: 4 October 2018

Accepted Date: 15 October 2018

Please cite this article as: Q. Ren, G. Yang, M. Guo, J. Guo, Y. Li, J. Lu, Q. Yang, H. Tang, Y. Li, X. Fang, Y. Sun, J.G. Qi, J. Tian, H. Wang, Design, synthesis, and discovery of ocotillol-type amide derivatives as orally available modulators of *P*-glycoprotein-mediated multidrug resistance, *European Journal of Medicinal Chemistry* (2018), doi: https://doi.org/10.1016/j.ejmech.2018.10.038.

Graphical Abstract

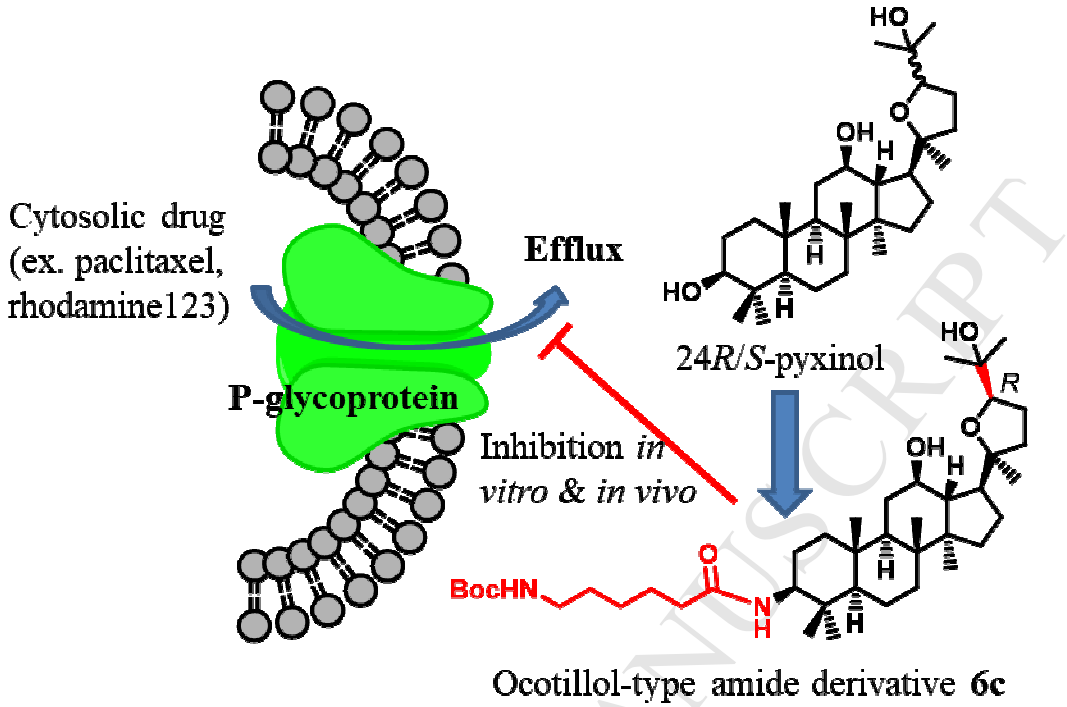

Docking score: **6c** (10.1319) > verapamil (8.3795) > pyxinol (4.8954)

Design, synthesis, and discovery of ocotillol-type amide derivatives as orally available modulators of P-glycoprotein-mediated multidrug resistance

Qianwen Ren[#a], Gangqiang Yang[#a*], Mengqi Guo[a,b], Jingwen Guo [a], Yang Li [a], Jing Lu [a], Qing Yang [a], Hanhan Tang [a], Yi Li [a], Xiaojuan Fang [a], Yixiao Sun [a], Jia Grace Qi [a], Jingwei Tian [a], Hongbo Wang [a *]

[a] School of Pharmacy, Collaborative Innovation Center of Advanced Drug Delivery System and Biotech Drugs in Universities of Shandong, Key Laboratory of Molecular Pharmacology and Drug Evaluation (Yantai University), Ministry of Education, Yantai University, Yantai, 264005, China

[b] State Key Laboratory of Bioactive Substances and Functions of Natural Medicines, Institute of Materia Medica, Chinese Academy of Medical Sciences and Peking Union Medical College, Beijing, 100050, China

[#] The authors contributed equally.

Corresponding authors : oceanygq@ytu.edu.cn (Gangqiang Yang), hongbowangyt@gmail.com (Hongbo Wang)

Keywords:

Ocotillol, P-glycoprotein modulators, Multidrug resistance reversal, Structure-active relationship, Molecular docking

Abstract: Multidrug resistance (MDR) is a major cause of failure in cancer treatment, in which the overexpression of P-glycoprotein (Pgp) plays a crucial role. Herein, a novel class of ocotillol-type amide derivatives has been designed, synthesized, and evaluated for their ability to reverse MDR. The structure-activity relationship of the reversal activity was analyzed. Ten compounds showed promising chemo-reversal ability, among which the 24*R*-ocotillol-type amide derivative **6c** with an *N*-Boc-hexanoyl unit exhibited the most potency in reversing paclitaxel resistance in KBV cells. Compound **6c** could inhibit Pgp-mediated rhodamine123 efflux function via stimulating Pgp-ATPase activity and exhibited high binding affinity with Pgp in molecular docking studies. Importantly, compound **6c** enhanced the efficacy of paclitaxel against KBV cancer cell-derived xenograft tumors in nude mice after oral administration. These results indicate that ocotillol-type amide derivatives are promising lead compounds for overcoming MDR in cancer.

1. Introduction

Multidrug resistance (MDR) is the major cause of the failure of cancer treatment in the clinic. In MDR, simultaneous resistance to anticancer drugs that are structurally and functionally unrelated is exhibited [1]. A primary mechanism of MDR results from the overproduction of P-glycoprotein (Pgp or ABCB1), the first identified drug efflux transporter in the plasma membrane [1]. With ATP consumption, Pgp can pump out anticancer drugs, such as paclitaxel and vinblastine, reducing the intracellular accumulation of anticancer drugs and avoiding their cytotoxic effects, which leads to poor clinical outcomes [2]. Therefore, one of the promising strategies for overcoming MDR is the development of Pgp modulators (inhibitors) able to reverse the MDR of cancer cells, reestablishing sensitivity to anticancer drugs [3]. A considerable number of Pgp modulators have been reported [4-5], such as the first-generation drug verapamil, second-generation dexverapamil and valspodar, and third-generation tariquidar and zosuquidar. However, none of these compounds are clinically available because of their intrinsic toxicity and pharmacokinetic issues [3, 5]. Thus, the discovery and development of effective Pgp modulators remains a great challenge.

The development of natural products is considered as a promising source for discovering the next generation of Pgp modulators, sometimes termed “the fourth generation inhibitors”, with high therapeutic efficacy and low toxicity [6]. Many nontoxic natural products have already been investigated to overcome MDR, such as diterpenoids, triterpenoids, cucurminoids, and flavonoids [4-5]. In particular, ginsenosides, the active chemical components extracted from *Panax ginseng*, exhibit

a range of biological effects, including anti-inflammatory, cytotoxic, antiproliferative, modulation of MDR, and antimicrobial activities [7]. In particular, protopanoxadiol ginsenosides Rg3 and Rh2 have been observed to reverse Pgp-mediated MDR [8-10]. The aglycone 20*S*-protopanoxadiol (PPD) and analogues have also been reported to have reversal effects on Pgp-mediated MDR cells [11-12]. Ocotillol-type ginsenosides, as distinguished from other ginsenosides, have the carbon chain at the C-20 position replaced by a tetrahydrofuran ring. These ginsenosides have been extensively studied for protective activity on the cardiovascular system [13-15], antitumor and antimicrobial activities [16-20], and as the main *in vivo* metabolites of ginsenosides [21-22]. However, there are few reports of ocotillol-type derivatives with MDR reversal activity.

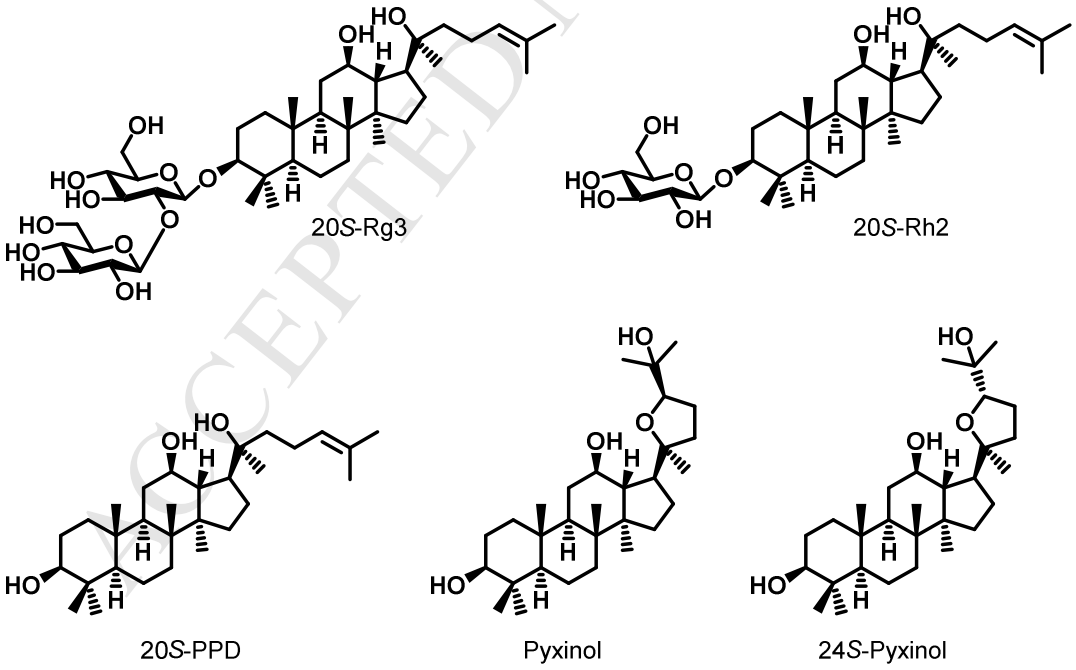

Fig. 1 Chemical structures of ginsenosides

In our search for MDR reversal agents from triterpenoid derivatives[23], we have prepared 29 new amide derivatives from pyxinol (**1**) and 24*S*-pyxinol (**2**), two

aglycones of ocotillol-type ginsenosides. Then the effects of these compounds on MDR reversal activity were evaluated with structure-activity relationship analysis. Compound **6c**, which showed the most potency, was investigated further with regard to its potency and mechanism of reversing Pgp-mediated MDR. The effect of compound **6c** *in vivo* was also validated in a KBV xenograft nude mice model.

2. Results and Discussion

2.1. Chemistry

On the basis of previous literature reports, the observed predominant metabolic pathway of pyxinol (**1**) and 24*S*-pyxinol (**2**) is oxidation of the C-3 hydroxy [21]. Therefore, the C-3 hydroxy was selected for further modification to block the predominant metabolic pathway. The preparation of the key intermediates **5** and **10**, in which the hydroxy group is substituted with an amine, is outlined in Scheme 1. The epimeric triols **1** and **2** were prepared by treating the commercially available PPD with 3-chloroperoxybenzoic acid (*m*-CPBA) as previously described [24]. Then, the oxidization of the C-3 hydroxy by pyridinium chlorochromate (PCC) and subsequent oximation gave the oxime. Oximes **4** and **9** were reduced to form the amines **5** and **10**, respectively.

To explore whether chemical modifications of the C-3 amine affect the MDR reversal ability, we synthesized a series of ocotillol-type amide derivatives (OADs) **6a**–**6l** and **11a**–**11h** containing an alkyl group, with or without, a terminal Boc-protected amine, aromatic ring, or heteroaromatic ring (Scheme 1). They were synthesized through amidation from **5** or **10** using corresponding acid in the presence

of *N*,*N*,*N*',*N*'-tetramethyl-*O*-(1H-benzotriazol-1-yl)uronium hexafluorophosphate (HBTU) and Et_3N. The OADs containing a Boc-protected amine were deprotected in the presence of trifluoroacetic acid to furnish compounds **7a**–**7e** and **12a**–**12d**.

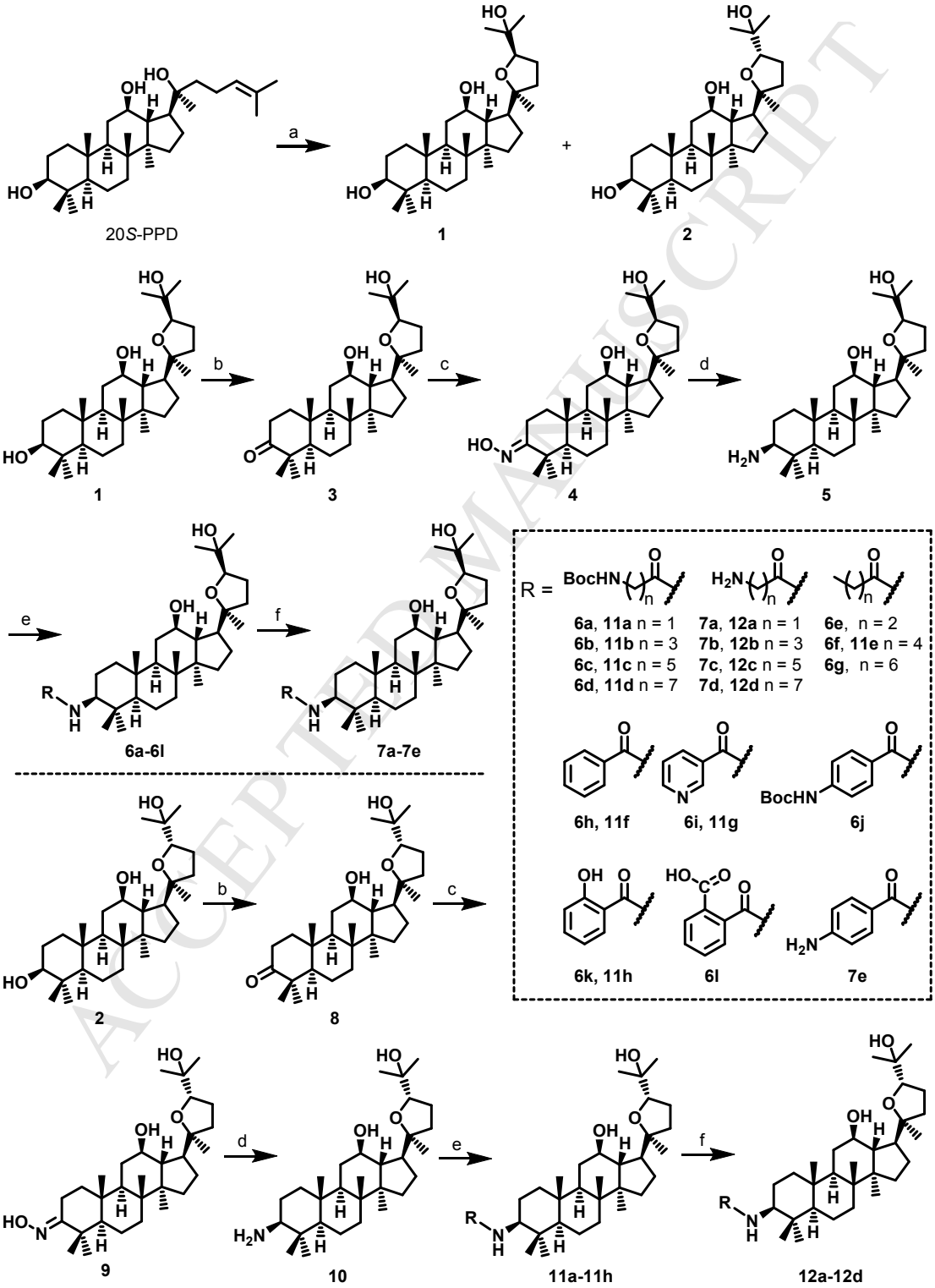

Scheme 1 synthesis of ocotillol-type amide derivatives (OADs)

Reagents and conditions: (a) *m*-CPBA, CH_2Cl_2, rt, 5 h; (b) PCC, CH_2Cl_2, 0 ºC to rt, 15 h; (c) Hydroxylamine hydrochloride, pyridine, 80 ºC, 3 h; (d) $NaCNBH_3$, $TiCl_3$, $AcONH_4$, *i*-PrOH, rt, 15 h; (e) 2-(Boc-amino)acetic acid, 4-(Boc-amino)butyric acid, 6-(Boc-amino)hexanoic acid, 8-(Boc-amino)octanoic acid, butyric acid, hexanoic acid, octanoic acid, benzoic acid, nicotinic acid, 4-(Boc-amino)benzoic acid, salicylic acid or phthalic acid, HBTU, NEt_3, DMF, rt, 0.5 h; (f) TFA, rt, 0.5 h.

2.2. Biological assays

2.2.1. *In vitro* cytotoxicity and the MDR reversal ability of OADs against paclitaxel resistance

The cytotoxicity and MDR reversal ability of all synthesized OADs were investigated in KBV cells, one common used MDR cell line, by the MTT method. As shown in Table 1, none of the OADs showed any appreciable toxicity in the KBV cells at a concentration of 10 μM. Then, the reversal ability was preliminarily evaluated at non-cytotoxic dosages of 10 and 5 μM. As expected, the synthesized OADs exhibited better MDR reversal ability than the aglycones of ocotillol-type ginsenosides (**1** and **2**). In summary, when co-administered with paclitaxel under the same conditions, half of the OADs exerted promising reversal ability compared with the classical Pgp modulator verapamil. Among these active compounds, compound **6c** showed the strongest reversal ability. Then, the MDR reversal potency and reversal fold (RF) values of **6c** were investigated. As shown in Table 2, at non-toxic concentrations, compound **6c,** as well as verapamil, dramatically decreased the IC_{50}

value of paclitaxel. The RF values of **6c** at concentrations of 5 and 10 μM were 27.97 and 47.85, respectively.

Based on the MDR reversal effects of the OADs on paclitaxel resistance, some structure activity relationship (SAR) correlations were proposed. As shown in Table 1, most 24*R*-derivatives (**5**, **6a**–**6l**, and **7a**–**7e**) exerted stronger MDR reversal abilities than the corresponding 24*S*-derivatives (**10**, **11a**–**11h**, and **12a**–**12d**). This result was in accordance with the results of a previous study [25], in which the effect of epimerization at the C-24 of ocotillol-type triterpenoids on the MDR reversal ability was first reported. The following trend in activity for the amide groups at the C-3 position of the 24*R*-derivatives was observed: linear alkyl amide containing terminal Boc-protected amine (**6a**–**6d**) > aromatic or heteroaromatic ring amide (**6h**–**6k** except for **6l**) > linear alkyl amide (**6e**–**6g**). Deprotection of Boc-protected amines obviously reduced the MDR reversal ability (**6a**–**6d** vs **7a**–**7d**). A length of six carbon atoms in the alkyl chain of the linear alkyl amide is preferred, whether the *N*-terminus is Boc-protected or not (**6c** and **6g**). Similar trends in activity were also found for the 24*S*-derivatives.

Table 1 The effect of novel ocotillol-type amide derivatives (OADs) on the cytotoxic activity of paclitaxel against KBV cells.[a]

Compound [b]	Cell survival (%)		
	Without paclitaxel	With paclitaxel (100 nM)	
	10 μM [c]	10 μM [c]	5 μM [c]
1	94 ± 2	95 ± 2	– [d]
5	125 ± 5	43 ± 1	72 ± 5
6a	95 ± 2	42 ± 3	48 ± 1
6b	67 ± 5	34 ± 1	48 ± 3

6c	128 ± 6	34 ± 3	46 ± 2
6d	106 ± 6	39 ± 1	54 ± 6
7a	103 ± 4	49 ± 3	99 ± 22
7b	77 ± 1	85 ± 5	100 ± 6
7c	86 ± 5	91 ± 14	91 ± 6
7d	80 ± 1	38 ± 4	84 ± 12
6e	103 ± 4	55 ± 2	89 ± 1
6f	101 ± 20	43 ± 1	69 ± 8
6g	70 ± 2	39 ± 1	56 ± 3
6h	101 ± 3	39 ± 2	59 ± 3
6i	87 ± 17	49 ± 2	55 ± 5
6j	77 ± 2	46 ± 3	54 ± 5
7e	75 ± 2	47 ± 2	77 ± 12
6k	100 ± 17	40 ± 2	51 ± 6
6l	105 ± 19	85 ± 7	96 ± 3
2	111 ± 5	104 ± 7	–
10	91 ± 7	88 ± 7	102 ± 5
11a	96 ± 11	42 ± 1	61 ± 3
11b	94 ± 1	44 ± 13	90 ± 3
11c	79 ± 6	40 ± 2	65 ± 1
11d	111 ± 5	41 ± 5	54 ± 2
12a	90 ± 10	115 ± 5	98 ± 7
12b	105 ± 5	102 ± 11	111 ± 3
12c	79 ± 4	101 ± 4	105 ± 7
12d	118 ± 4	76 ± 8	118 ± 8
11e	98 ± 8	44 ± 0	78 ± 12
11f	116 ± 8	48 ± 5	90 ± 12
11g	91 ± 6	61 ± 6	115 ± 12
11h	96 ± 13	36 ± 1	61 ± 6
DMSO [e]	–	104 ± 8	–
verapamil	–	43 ± 6	–

[a] n = 1–3 independent experiments, and the values are presented as the mean ± SD. The known Pgp inhibitor verapamil was included for comparison.

[b] All compounds were dissolved in DMSO for testing.

[c] Compounds at 10 or 5 μM.

[d] Not determined.

[e] DMSO was used as solvent control.

Table 2 Drug resistance reversal ability of selected compounds in KBV cells.

Treatment	IC_{50} ± SD [a] (nM)	RF [b]
Paclitaxel	1353.98 ± 303.33	1.00
+ 5 μM **5**	135.40 ± 30.33	10.00
+ 10 μM **5**	48.16 ± 11.08	28.11
+ 5 μM **6c**	48.41 ± 3.16	27.97
+ 10 μM **6c**	28.29 ± 2.90	47.85
+ 10 μM Verapamil	28.16 ± 7.26	48.08

[a] IC_{50} values are represented as mean ± SD (n = 3).

[b] The reversal fold (RF) value was calculated as the ratio between the IC_{50} values for paclitaxel in KBV cells without and with inhibitor.

In summary, compound **6c**, which exhibited the strongest MDR reversal ability, is a promising lead compound for drug development and is worthy of more detailed studies.

2.2.2. Effects of **6c** on paclitaxel-induced cell cycle arrest and cell apoptosis in KBV cells

Paclitaxel is well-known to induce cell cycle arrest at the G_2-M phase, leading to cell apoptosis[26]. To evaluate whether **6c** can enhance paclitaxel-induced apoptosis and cell cycle arrest in MDR cells, we analyzed the cell cycle distribution of KVB cells by flow cytometry (Fig. 2 and Table 3). Similar to verapamil (the positive control, 10 μM), compound **6c** (5 μM) significantly increased the population of paclitaxel-treated cells in the G_2-M phase ($p < 0.01$), while the percentage of cells in the G_1-G_0 phase was reduced. The cell apoptotic portion, indicated by the ratio of cells in the sub-G_1 phase, was increased to 43.12% ± 1.67% and 43.98% ± 0.39% in

paclitaxel-treated cells by treatment with **6c** and verapamil, respectively, after 24-h culture (Fig. 2 and Table 3).

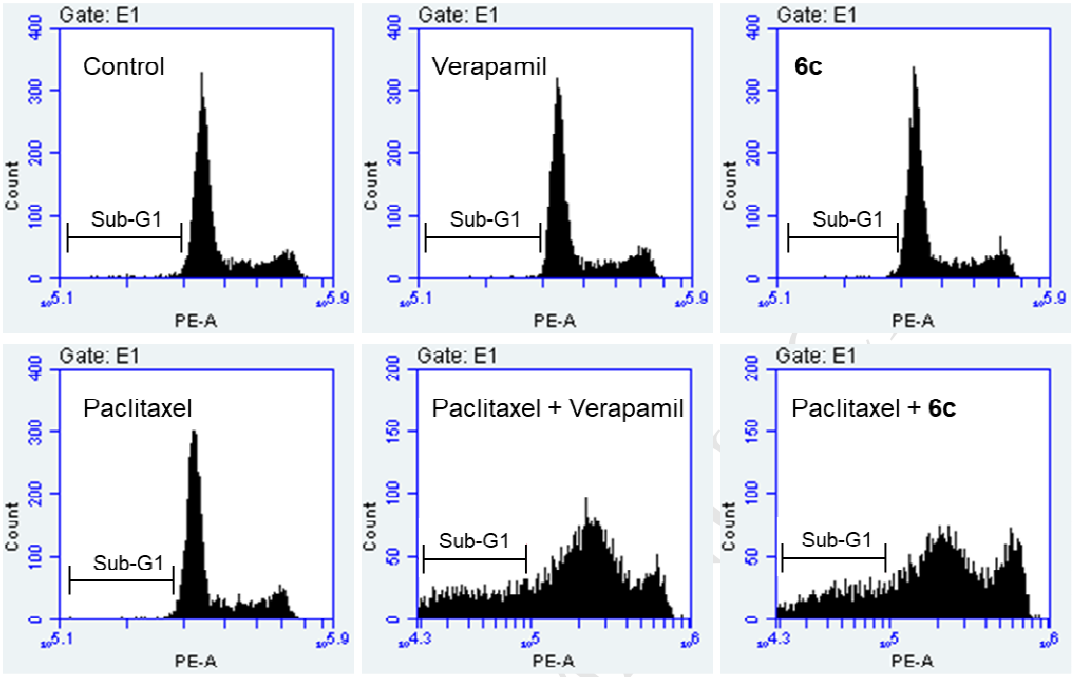

Fig. 2 Effect of **6c** on paclitaxel activity in cell cycle distribution and apoptosis

Cells were seeded into 6-well plates at 3×10^5 KBV cells per well and treated with test compounds for 24 h. The cells were then subjected to flow cytometry assay to determine the cell cycle and analyzed.

Table 3 Effect of **6c** on paclitaxel activity in cell cycle distribution and apoptosis

Treatment (μM)	Sub-G_1 (%)	G_1-G_0 (%)	S (%)	G_2-M (%)
Control	2.21 ± 1.02	70.35 ± 0.79	10.03 ± 0.75	19.62 ± 1.54
Ptx (0.1)	2.29 ± 0.39	71.11 ± 2.00	12.54 ± 4.01	16.35 ± 2.02
Vrp (10)	2.25 ± 0.69	68.09 ± 2.25	9.99 ± 0.41	21.92 ± 1.85
Vrp (10) + Ptx (0.1)	43.98 ± 0.39**	58.54 ± 1.05**	15.46 ± 0.73	26.00 ± 0.83**
6c (10)	2.35 ± 0.24	73.29 ± 1.58	9.22 ± 0.61	17.49 ± 1.21
6c (5) + Ptx (0.1)	43.12 ± 1.67**	44.52 ± 0.80**	16.05 ± 0.78	39.43 ± 1.02**

All data were expressed as mean ± SD (n = 3). **: $p < 0.01$, *: $p < 0.05$, compared with control group. Ptx, paclitaxel; Vrp, verapamil.

2.2.3. Inhibition of Rhodamine123 efflux mediated by Pgp

Rhodamine123, a well-known Pgp substrate, has been widely used as a biomarker to assess the ability of MDR reversal agents on Pgp efflux function [23]. To investigate whether compound **6c** can interfere with Pgp function, the effect of **6c** on the inhibition of Rhodamine123 efflux was tested in KBV cells. Verapamil was used as the positive control. As shown in Fig. 3, treatment with **6c** increased the accumulation of Rhodamine123 in KBV cells in a dose-dependent manner. In particular, the accumulation of Rhodamine123 in KBV cells treated with **6c**, even at 2 μM, was higher than in KBV cells treated with verapamil at 10 μM. These results suggested that **6c** is a promising modulator of Pgp efflux pump activity.

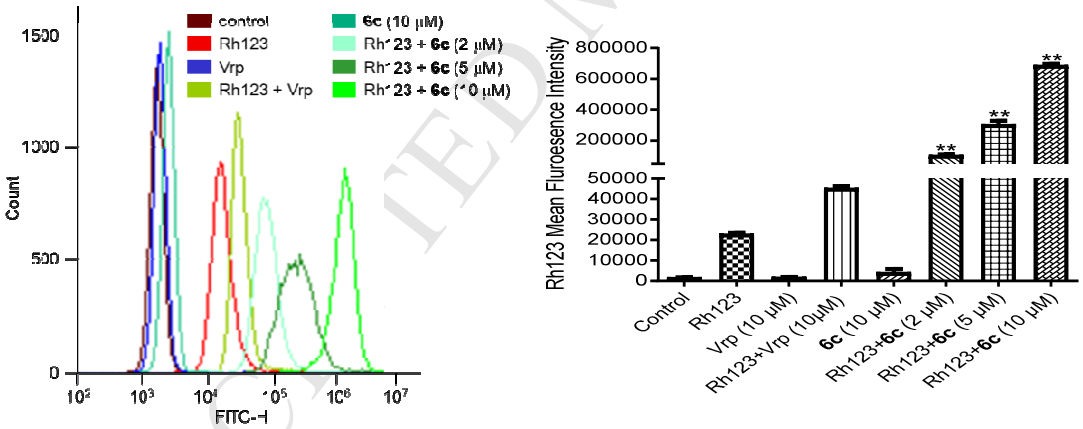

Fig. 3. Effect of compound **6c** on Pgp activity in KBV cells.

Cells were incubated with Rhodamine123 in the presence or absence of test compounds, and then harvested for analysis by flow cytometry. Rh123: Rhodamine123; Vrp: Verapamil. All data were presented as mean ± SD (n =3). * *: $p < 0.01$, compared with control group.

2.2.4. Effect of compound **6c** on Pgp-ATPase activity

The effect of **6c** on Pgp-ATPase activity was further determined using the Pgp-Glo™ assay. Verapamil, a modulator as well as a substrate of Pgp, was used as the positive control. At 0.5 mM, compound **6c** and verapamil increased the Pgp-ATPase activity over the basal level by 6.03- and 10.78-fold, respectively (Fig. 4). Both **6c** and verapamil significantly increased the ATP consumption in a dose-dependent manner ($p < 0.01$). These results revealed that, similar to verapamil, compound **6c** can stimulate Pgp-ATPase activity.

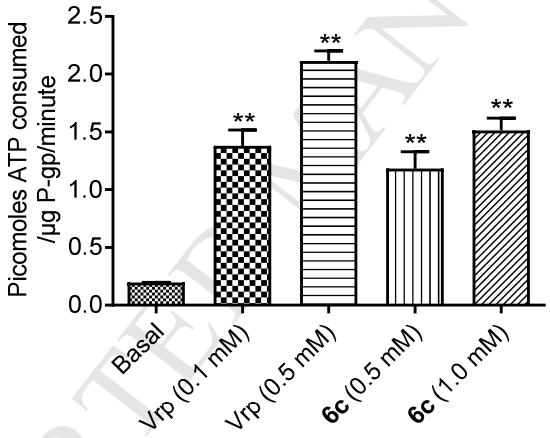

Fig.4. Effect of compound **6c** on the Pgp-ATPase activity. Purified Pgp was incubated with test compounds, and the luminescence was measured. Vrp: Verapamil. All data were presented by means ± SD (n=3). **: $p < 0.01$, compared with that in basal group.

2.2.5. Molecular modeling

To further understand the interaction between the OADs and Pgp, compounds **6c**, **5**, **1**, and verapamil (the positive control) were subjected to in silico analysis with a

homology model of human Pgp [27]. Compound **6c** was predicted to bind into the large drug-binding cavity inside the transmembrane domains of human Pgp through hydrophobic interactions with nearby residues (Fig. 5A). The hydroxy group at C-25 interacted with the side-chain hydroxy group of Thr199 to form a hydrogen bond (2.59 □). The oxygen atom in the furan ring formed another hydrogen bond with the side-chain amino group of Gln347 (>O⋯H_2N-Gln347, 3.19 Å). Compound **6c** exhibited a high binding affinity with a docking score of 10.1319, much higher than verapamil (Table 4). The order of the binding affinity of selected compounds as indicated by the docking score was: **6c** > verapamil **> 5** > **1**. These results were essentially in agreement with the reversal MDR ability exhibited in KBV cells, as well as the inhibition of Rhodamine123 efflux.

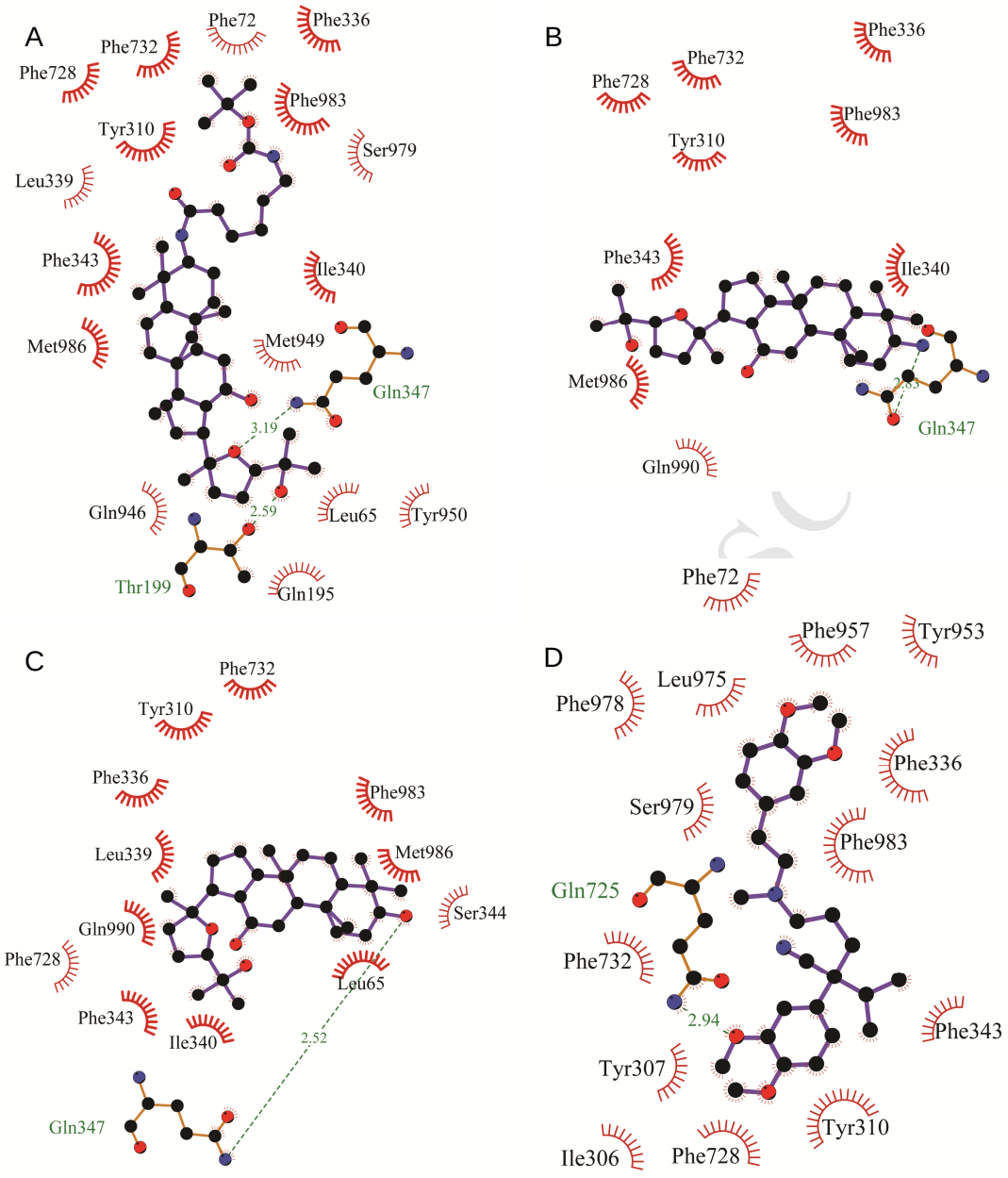

Fig.5 Molecular modeling of **6c**, **5**, **1**, and verapamil binding to human Pgp. The Surflex-Dock module in SYBYL-X2.1.1 was used to analyze the interactions between (A) **6c**, (B) **5**, (C) **1**, and (D) verapamil and the protein residues of human Pgp. Hydrogen bonds and hydrophobic interactions are shown as green dashed lines and red “eyelashes”, respectively. The figures were generated using LIGPLOT v.1.4.5.

Table 4 Scores of the docking models of Pgp and **6c**, **5**, **1**, and verapamil.

Compound	Total score	Crash	Polar
6c	10.1319	-3.5341	1.5004
5	6.2148	-1.3739	1.2048
1	4.8954	-4.3954	0.4267
Verapamil	8.3795	-1.8429	1.1060

2.2.6. *In vivo* evaluation

The xenograft tumors of KBV were established using nude mice to explore the effect of compound **6c** on the antitumor activity of paclitaxel *in vivo*. Consistent with the results in the cell model, the xenograft tumors of KBV were also resistant to paclitaxel, at a dosage of 30 mg/kg (Fig. 6). Co-treatment with compound **6c** via oral administration at a dosage of 10 mg/kg, significantly increased the tumor inhibitory activity of paclitaxel ($p < 0.05$), although compound **6c** alone did not show any obvious antitumor activity (Fig. 6, Table 5). The increased toxicity of the combination therapy, which was indicated by a loss in body weight, could still be tolerated based on all the animals surviving at the end of the experiments (Table 5). These results indicated that, as a potent Pgp modulator, compound **6c** could efficiently restore the chemosensitivity of MDR human tumors to paclitaxel at a tolerated dose.

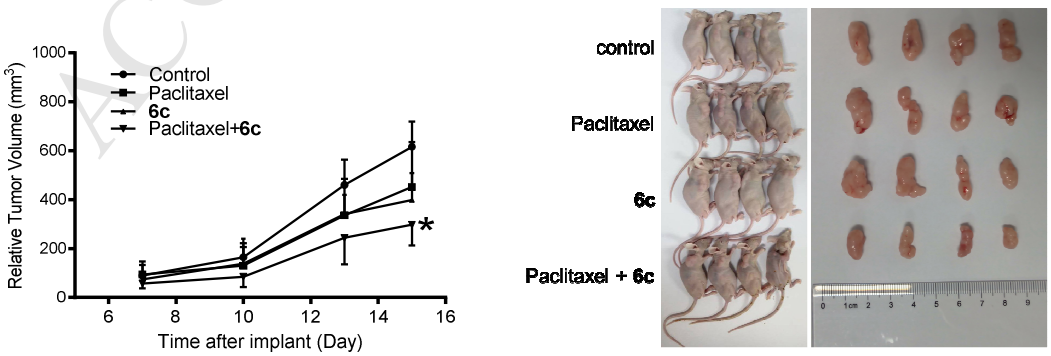

Fig 6 Effect of compound **6c** on the antitumor activity of paclitaxel in KBV

xenotransplants in nude mice.

The animals were injected with KBV cells and treated with the indicated compounds. After 2 weeks of administration, the nude mice were euthanized and the tumors were peeled off and weighed. All data were presented as mean ± SD (n = 4). *: $p < 0.05$, compared with control group.

Table 5 Effect of compound **6c** on the antitumor activity of paclitaxel on KBV xenotransplants in nude mice.

Group (mg/kg)	Number (Initial/End)	Body weight (g)		Tumor weight (g)	
		Initial	End	g	IR (%)
Control	4/4	19.84 ± 0.86	20.92 ± 2.29	0.67 ± 0.079	
Paclitaxel (30)	4/4	20.24 ± 1.14	18.88 ± 1.75	0.55 ± 0.20	17.90
6c (10)	4/4	20,62 ± 0.81	21.85 ± 0.88	0.60 ± 0.30	10.45
Paclitaxel + **6c**	4/4	19.88 ± 0.74	15.98 ± 2.21*	0.31 ± 0.11*	53.73

IR: inhibition ratio. *: $P < 0.05$, compared with control group.

3 Conclusions

Ocotillol-type derivatives have been reported to be potential Pgp modulators [25, 28]. However, because limited numbers of these derivatives are available, very little SAR and biological information is known. In the current study, we designed and synthesized a series of OADs from the rare natural products pyxinol (**1**) and 24*S*-pyxinol (**2**). The *in vitro* MDR reversal abilities of these new derivatives were investigated in KBV cells. SAR studies indicated that most 24*R*-derivatives exerted stronger MDR reversal abilities than the corresponding 24*S*-derivatives (Table 1). SAR studies also revealed that the order of activity for the amide groups at C-3 was: linear alkyl amide containing a terminal Boc-protected amine > aromatic or heteroaromatic ring amide > linear alkyl amide > linear alkyl amide containing a

terminal amine. In addition, a chain length of six carbon atoms in the linear alkyl amide was preferred. These results indicated that the length and hydrophobicity of the amide group at C-3 is important for activity. These results were supported by the molecular modeling results as shown in Fig. 5. Biological evaluation *in vitro* demonstrated that a few of the OADs exerted promising reversal ability compared with the classical Pgp modulator, verapamil. In particular, compound **6c** showed considerable MDR reversal ability at a non-toxic concentration and enhanced paclitaxel-induced apoptosis and cell cycle arrest at the G_2-M phase in KBV cells overexpressing Pgp (Fig. 2 and Table 3).

Compound **6c** showed a remarkable capacity for inhibiting the Pgp-mediated drug efflux of Rhodamine123 in KBV cells, superior to verapamil (Fig. 3). Results of a western blot assay indicated that the reversal ability of **6c** on Pgp-mediated MDR was not because of decreased protein expression of Pgp (data not shown). Thus, whether the reversal ability of **6c** was because of inhibition of the Pgp function was further confirmed. Results of the Pgp-ATPase activity assay revealed that **6c** could stimulate Pgp-ATPase activity, but not as strongly as verapamil. Further molecular modeling analysis of the binding interactions between **6c** and Pgp suggested that **6c**, as well as verapamil, bind into the drug-binding cavity inside the trasmembrane domains of human Pgp (Fig. 5). The docking scores showed that **6c** has a much higher binding affinity with Pgp than verapamil (Table 4). The differences between **6c** and verapamil in the intracellular Rhodamine123 accumulation assay and Pgp-ATPase activity assay might be because of their different binding affinities, which affect their capacity to

release from Pgp. These results demonstrated that **6c** can be considered as a potential modulator of Pgp.

In addition, we investigated the effect of **6c** on the antitumor activity of paclitaxel *in vivo* in a nude mouse xenograft model. Orally administrated **6c** remarkably enhanced the tumor inhibitory activity of paclitaxel at a tolerated dose (Fig. 6, Table 5). These results validated **6c** as a promising Pgp modulator to efficiently restore the chemosensitivity of MDR human tumors to paclitaxel.

The present study demonstrated that the novel ocotillol-type derivative **6c** exhibited potential in reversing Pgp-mediated MDR *in vitro* and *in vivo*. This compound is a promising lead for the development of new MDR reversal agents. Further investigations on several pharmaceutical issues, including the drug safety, the drug–drug interactions in combination therapy, and the *in vivo* pharmacokinetics will be undertaken in the future.

4. Experimental section

4.1 General

Unless otherwise stated, reactions were performed in flame-dried glassware under an argon atmosphere using dry solvents. Solvents were dried over activated molecular sieves under argon. All the starting materials were purchased from commercial sources and used as received, unless otherwise stated. Liquids and solutions were transferred via syringe or positive-pressure cannula. Brine solutions refer to saturated aqueous sodium chloride solutions. Thin-layer chromatography (TLC) was performed using silica gel 60 F_{254} precoated plates (0.25 mm) and visualized by UV fluorescence

quenching, anisaldehyde, or $H_3(PMo_{12}O_{40})$ staining. Silica gel (200-300 mesh, Qingdao Marine Chemical Co. Ltd., China) was used for column chromatography. ^1H and ^{13}C NMR spectra were recorded on ECA400 spectrometers (JEOL Ltd.) and chemical shifts are given in parts per million (ppm) relative to Me_4Si (^1H: 0.0 ppm) in $CDCl_3$ (^{13}C: 77.0 ppm) or CD_2HOD in CD_3OD (^1H: 3.30 ppm, ^{13}C: 49.0 ppm). Data for ^1H NMR spectra are reported as follows: chemical shift (ppm) (multiplicity, coupling constant (Hz), integration). Multiplicity and qualifier abbreviations are as follows: s = singlet, d = doublet, t = triplet, q = quartet, quint = quintet, m = multiplet, br = broad. High-resolution mass spectra (HRMS) were recorded by using Thermo Scientific Q Exactive mass spectrometer. Optical rotation was recorded on a SGW-3 spectrometer.

4.2 The synthesis of compound **5** and **10**

4.2.1 (20*S*, 24*R*)-Epoxy-dammarane-3*β*, 12*β*, 25-triol (**1**) and (20*S*, 24*S*)-Epoxy-dammarane-3*β*, 12*β*, 25-triol (**2**)

Compound **1** and **2** were prepared from commercially available PPD according to the published procedures [24].

4.2.2 (20*S*, 24*R*)-Epoxy-12*β*, 25-dihydroxy-dammarane-3-one (**3**) and (20*S*, 24*S*)-Epoxy-12*β*, 25-dihydroxy-dammarane-3-one (**8**)

Compound **3** (or **8**) was prepared from the oxidation of **1** (or **2**) according to the published procedures[19].

4.2.3 (20*S*, 24*R*)-Epoxy-12*β*, 25-dihydroxy-dammarane-3-one oxime (**4**)

To a solution of **3** (2.000 g, 4.213 mmol) in pyridine (40 mL) was added hydroxylamine hydrochloride (0.439 g, 6.317 mmol). After being stirred for 3 h at 80 ºC, the reaction mixture was diluted with H_2O and extracted with EtOAc. The combined organic layer was washed with brine, dried over Na_2SO_4, filtered, concentrated, and purified by silica gel column chromatography to provide the oxime **4** (2.028 g, 4.141 mmol, 98%) as a white solid.

M.p. 251-252 ºC; $[\alpha]_D^{26}$ +8.8 (*c* 1.0, $CHCl_3$); ^{1}H NMR (400 MHz, $CDCl_3$) δ 5.61 (s, 1H), 3.85 (dd, *J* = 8.9, 6.6 Hz, 1H), 3.51 (td, *J* = 10.5, 4.6 Hz, 1H), 2.99 (ddd, *J* = 15.5, 5.9, 4.1 Hz, 1H), 2.27 (ddd, *J* = 15.5, 11.4, 5.9 Hz, 1H), 2.19 (td, *J* = 10.1, 3.0 Hz, 1H), 2.09-1.79 (m, 6H), 1.71-1.41 (m, 7H), 1.34-0.73 (m, 6H), 1.28 (s, 3H), 1.27 (s, 3H), 1.14 (s, 3H), 1.10 (s, 3H), 1.05 (s, 3H), 1.01 (s, 3H), 0.96 (s, 3H), 0.88 (s, 3H); ^{13}C NMR (100 MHz, $CDCl_3$) δ 166.9, 86.5, 85.4, 70.9, 70.1, 56.2, 52.0, 50.1, 49.4, 47.9, 40.4, 39.7, 39.0, 37.2, 34.4, 32.6, 31.5, 31.2, 28.6, 27.9, 27.6, 27.3, 26.1, 25.0, 22.7, 19.0, 18.0, 17.0, 16.0, 15.3. HRMS (ESI, positive) *m/z* $[M+H]^+$ calcd for $C_{30}H_{52}N_1O_4$ 490.3891, found 490.3900.

4.2.4 (20*S*, 24*R*)-Epoxy-3*β*-amino-dammarane-12*β*, 25-diol (**5**)

To a solution of **4** (800 mg, 1.63 mmol), $NaCNBH_3$ (258 mg, 4.11 mmol) and $AcONH_4$ (315 mg, 4.09 mmol) in *i*-PrOH (50 mL) was added 15% $TiCl_3$ aq (1.6 mL) at 0 □. After being stirred for 15 h at rt, the reaction mixture was diluted with H_2O

and extracted with EtOAc. The combined organic layer was washed with brine, dried over Na_2SO_4, filtered and concentrated. The residue was recrystallized from hot MeOH to obtain **5** (545 mg, 1.15 mmol, 70%) as a white powder.

M.p. 268-269 ºC; $[\alpha]_D^{13}$ +22.4 (*c* 1.0, $CHCl_3$); ^{1}H NMR (400 MHz, $CDCl_3$) δ 3.84 (dd, *J* = 8.4, 6.8 Hz, 1H), 3.51 (td, *J* = 10.4, 4.3 Hz, 1H), 2.85 (dd, *J* = 10.6, 5.8 Hz, 1H), 2.18 (td, *J* = 10.0, 3.4 Hz, 1H), 2.09 - 1.96 (m, 2H), 1.92 – 1.26 (m, 16H), 1.27 (s, 3H), 1.26 (s, 3H), 1.11 – 1.05 (m, 1H), 1.13 (s, 3H), 1.09 (s, 3H), 0.98 (s, 3H), 0.98 – 0.92 (m, 1H), 0.95 (s, 3H), 0.89 (s, 3H), 0.87 (s, 3H), 0.78 (d, *J* = 9.2 Hz, 1H); ^{13}C NMR (100 MHz, $CDCl_3$) δ 86.5, 85.4, 70.8, 70.1, 60.7, 56.4, 52.0, 50.3, 49.3, 47.9, 39.7, 38.6, 37.0, 36.9, 34.6, 32.6, 31.2, 31.2, 28.5 (2C), 27.9, 27.5, 26.1, 25.0, 23.6, 18.2, 18.1, 16.3, 16.0, 15.4. HRMS (ESI, positive) *m/z* $[M+H]^+$ calcd for $C_{30}H_{54}N_1O_3$ 476.4098, found 476.4079.

4.2.5 (20*S*, 24*S*)-Epoxy-12*β*, 25-dihydroxy-dammarane-3-one oxime (**9**)

To a solution of **8** (1.245 g, 2.622 mmol) in pyridine was added hydroxylamine hydrochloride (0.314 g, 4.519 mmol). After being stirred for 3 h at 80 ºC, the reaction mixture was diluted with H_2O and extracted with EtOAc. The combined organic layer was washed with brine, dried over Na_2SO_4, filtered, concentrated, and purified by silica gel column chromatography to provide the oxime **9** (1.123 g, 2.295 mmol, 87%) as a white solid.

M.p. 206-207 ºC;$[\alpha]_D^{19}$ -2.4 (*c* 1.0, $CHCl_3$); ^{1}H NMR (400 MHz, $CDCl_3$) δ 5.78 (s, 1H), 3.89 (dd, *J* = 10.7, 5.3 Hz, 1H), 3.53 (td, *J* = 10.4, 4.7 Hz, 1H), 2.98 (ddd, *J* =

15.6, 5.7, 3.9 Hz, 1H), 2.34-2.22 (m, 2H), 2.06 (td, *J* = 11.1, 4.7 Hz, 1H), 2.01-1.82 (m, 5H), 1.77 (dd, *J* = 11.4, 6.9 Hz, 1H), 1.70 (t, *J* = 10.1 Hz, 1H), 1.56-1.49 (m, 5H), 1.34-1.09 (m, 6H), 1.28 (s, 3H), 1.24 (s, 3H), 1.15 (s, 3H), 1.11 (s, 3H), 1.07 (s, 3H), 1.04 (s, 3H), 0.98 (s, 3H), 0.90 (s, 3H); ^{13}C NMR (100 MHz, $CDCl_3$) δ 166.9, 87.4, 87.1, 70.4, 70.0, 56.0, 52.1, 49.8, 48.9, 48.8, 40.3, 39.7, 38.9, 37.2, 34.3, 32.1, 31.8, 31.6, 28.8, 28.5, 28.0, 27.3, 25.0, 24.2, 22.7, 19.0, 17.6, 17.1, 15.9, 15.3. HRMS (ESI, positive) *m/z* $[M+H]^+$ calcd for $C_{30}H_{52}N_1O_4$ 490.3891, found 490.3899.

4.2.6 (20*S*, 24*S*)-Epoxy-3*β*-amino-dammarane-12*β*, 25-diol (**10**)

To a solution of **9** (533 mg, 1.09 mmol), $NaCNBH_3$ (172 mg, 2.74 mmol) and $AcONH_4$ (210 mg, 2.72 mmol) in *i*-PrOH (40 mL) was added 15% $TiCl_3$ aq (1.04 mL) at 0 □. After being stirred for 15 h at rt, the reaction mixture was diluted with H_2O and extracted with EtOAc. The combined organic layer was washed with brine, dried over Na_2SO_4, filtered and concentrated. The residue was recrystallized from hot MeOH to obtain **10** (342 mg, 0.719 mmol, 66%) as a white powder.

M.p. 265-266 ºC; $[\alpha]_D^{21}$ +4.4 (*c* 1.0, MeOH); ^{1}H NMR (400 MHz, CD_3OD) δ 3.81 (dd, *J* = 10.3, 4.8 Hz, 1H), 3.50 (td, *J* = 10.3, 4.9 Hz, 1H), 2.91 (dd, *J* = 10.7, 5.7 Hz, 1H), 2.22 (td, *J* = 10.1, 3.5 Hz, 1H), 2.04-1.53 (m, 13H), 1.41-0.91 (m, 8H), 1.26 (s, 3H), 1.17 (s, 3H), 1.10 (s, 3H), 1.06 (s, 6H), 0.94 (s, 6H), 0.89 (s, 3H); ^{13}C NMR (100 MHz, CD_3OD) δ 89.0, 88.4, 71.9, 71.3, 61.3, 57.2, 53.2, 51.3, 50.2, 49.7, 40.9, 39.5, 38.2, 37.7, 35.6, 33.4, 32.8, 32.6, 29.4, 29.1, 28.2, 26.5, 26.2, 26.1, 24.4, 19.2, 18.3, 16.6, 16.2, 15.9. HRMS (ESI, positive) *m/z* $[M+H]^+$ calcd for $C_{30}H_{54}N_1O_3$ 476.4098,

found 476.4103.

4.3 General procedure for the synthesis of **6a-6l** and **11a-11h**

To a solution of the amine (**5** or **10**) (0.042 mmol) and corresponding acid (0.059 mmol) in dry DMF (0.4 mL), was added HBTU (22 mg, 0.068 mmol) and Et_3N (20 μL) at 0 □ under Ar. After being stirred for 10 min at rt，the reaction mixture was diluted with H_2O and extracted with EtOAc. The combined organic layer was washed with sat. $NaHCO_3$ aq and brine, dried over Na_2SO_4, filtered, concentrated, and purified by silica gel column chromatography to provide the compounds **6a-6l** and **11a-11h**.

TFA (0.5 mL) was added to **6a** (or **6b**, **6c**, **6d**, **6j**, **11a**, **11b**, **11c**, **11d**) (0.03 mmol) at 0 ℃. After being stirring for 10 min at rt, the reaction mixture was concentrated to provide compounds **7a-7e** and **12a-12d**.

4.3.1 (20*S*, 24*R*)-Epoxy-3*β*-*N*-(2-Boc-aminoacetyl)-dammarane-12*β*, 25-diol (**6a**)

Yield：90%; $[\alpha]_D^{29}$ +16.4 (*c* 1.0, $CHCl_3$); ^{1}H NMR (400 MHz, $CDCl_3$) δ 6.07 (d, *J* = 9.6 Hz, 1H), 3.85 (dd, *J* = 8.9, 6.6 Hz, 1H), 3.78 (dd, *J* = 16.5, 5.9 Hz, 1H), 3.71 (dd, *J* = 16.5, 5.9 Hz, 1H), 3.67-3.60 (m, 1H), 3.49 (td, *J* = 10.5, 4.6 Hz, 1H), 2.19 (td, *J* = 10.1, 3.2 Hz, 1H), 2.08-0.88 (m, 21H), 1.45 (s, 9H), 1.28 (s, 3H), 1.27 (s, 3H), 1.09 (s, 3H), 0.98 (s, 3H), 0.90 (s, 3H), 0.86 (s, 3H), 0.83 (s, 3H), 0.76 (s, 3H); ^{13}C NMR (100 MHz, $CDCl_3$) δ 168.9, 156.1, 86.5, 85.4, 80.3, 70.9, 70.1, 56.6, 56.5, 52.0, 50.4, 49.4, 47.9, 44.9, 39.7, 39.3, 37.9, 37.0, 34.7, 32.6, 31.2, 31.2, 28.6, 28.3, 28.3 (3C), 27.9, 27.6, 26.1, 25.4, 25.0, 18.5, 18.1, 16.2, 16.1, 15.3. HRMS (ESI, positive) *m/z* $[M+H]^+$

calcd for $C_{37}H_{65}N_2O_6$ 633.4837, found 633.4846.

4.3.2 (20*S*, 24*R*)-Epoxy-3*β*-*N*-(4-Boc-aminobutyryl)-dammarane-12*β*, 25-diol (**6b**)

Yield, 97%; $[\alpha]_D^{30}$ +13.8 (*c* 1.0, $CHCl_3$); ^{1}H NMR (400 MHz, $CDCl_3$) δ 5.97 (d, *J* = 9.6 Hz, 1H), 4.80 (t, *J* = 6.2 Hz, 1H), 3.85 (dd, *J* = 8.7, 6.9 Hz, 1H), 3.65 (td, *J* = 10.7, 5.0 Hz, 1H), 3.52 (td, *J* = 10.5, 4.6 Hz, 1H), 3.23-3.10 (m, 2H), 2.23-2.16 (3H), 2.08-0.88 (m, 23H), 1.43 (s, 9H), 1.28 (s, 3H), 1.27 (s, 3H), 1.09 (s, 3H), 0.98 (s, 3H), 0.90 (s, 3H), 0.86 (s, 3H), 0.85 (s, 3H), 0.78 (s, 3H); ^{13}C NMR (100 MHz, $CDCl_3$) δ 172.1, 156.5, 86.5, 85.4, 79.3, 70.9, 70.1, 56.7, 56.5, 52.0, 50.4, 49.4, 47.9, 39.7 (2C), 39.4, 37.8, 37.0, 34.7, 34.1, 32.6, 31.2, 31.2, 28.6, 28.4, 28.4 (3C), 27.9, 27.6, 26.7, 26.1, 25.6, 25.0, 18.5, 18.1, 16.3, 16.2, 15.3. HRMS (ESI, positive) *m/z* $[M+H]^+$ calcd for $C_{39}H_{69}N_2O_6$ 661.5150, found 661.5161.

4.3.3 (20*S*, 24*R*)-Epoxy-3*β*-*N*-(6-Boc-aminohexanoyl)-dammarane-12*β*, 25-diol (**6c**)

Yield, 91%; $[\alpha]_D^{25}$ +12.9 (*c* 1.0, $CHCl_3$); ^{1}H NMR (400 MHz, $CDCl_3$) δ 5.44 (d, *J* = 9.6 Hz, 1H), 4.63 (s, 1H), 3.85 (dd, *J* = 8.9, 6.6 Hz, 1H), 3.66 (ddd, *J* = 11.9, 10.1, 4.12 Hz, 1H), 3.51 (td, *J* = 10.5, 4.6 Hz, 1H), 3.13-3.07 (m, 2H), 2.81 (s, 1H), 2.22-2.16 (m, 3H), 2.08-1.83 (m, 5H), 1.70-0.88 (m, 22H), 1.44 (s, 9H), 1.27 (s, 3H), 1.27 (s, 3H), 1.09 (s, 3H), 0.98 (s, 3H), 0.90 (s, 3H), 0.86 (s, 3H), 0.84 (s, 3H), 0.76 (s, 3H); ^{13}C NMR (100 MHz, $CDCl_3$) δ 172.3, 155.9, 86.4, 85.3, 78.9, 70.9, 70.0, 56.6, 56.2, 51.9, 50.3, 49.3, 47.8, 40.2, 39.6, 39.3, 37.7, 36.9, 36.9, 34.6, 32.5, 31.2, 31.1, 28.5, 28.3 (5C), 27.8, 27.5, 26.3, 26.0, 25.6, 25.4, 24.9, 18.4, 18.1, 16.3, 16.1, 15.3.

HRMS (ESI, positive) *m/z* $[M+H]^+$ calcd for $C_{41}H_{73}N_2O_6$ 689.5463, found 689.5474.

4.3.4 (20*S*, 24*R*)-Epoxy-3*β*-*N*-(8-Boc-aminooctanoyl)-dammarane-12*β*, 25-diol (**6d**)

Yield, 90%; $[\alpha]_D^{31}$ +15.7 (*c* 1.0, $CHCl_3$); ^{1}H NMR (400 MHz, $CDCl_3$) δ 5.29 (d, *J* = 10.1 Hz, 1H), 4.53 (s, 1H), 3.85 (dd, *J* = 8.9, 6.6 Hz, 1H), 3.66 (ddd, *J* = 12.3, 10.1, 4.6 Hz, 1H), 3.52 (td, *J* = 10.5, 4.6 Hz, 1H), 3.09 (dd, *J* = 7.3, 6.4 Hz, 2H), 2.22-2.14 (m, 3H), 2.08-1.83 (m, 5H), 1.71-0.77 (m, 23H), 1.44 (s, 9H), 1.28 (s, 3H), 1.27 (s, 3H), 1.09 (s, 3H), 0.98 (s, 3H), 0.90 (s, 3H), 0.86 (s, 3H), 0.84 (s, 3H), 0.76 (s, 3H); ^{13}C NMR (100 MHz, $CDCl_3$) δ 172.5, 156.0, 86.5, 85.4, 79.0, 70.9, 70.1, 56.6, 56.2, 52.0, 50.4, 49.4, 47.9, 40.5, 39.7, 39.4, 37.8, 37.1, 37.0, 34.7, 32.6, 31.2, 31.2, 29.9, 29.1, 28.9, 28.6, 28.4 (4C), 27.9, 27.6, 26.5, 26.1, 25.8, 25.7, 25.0, 18.5, 18.1, 16.3, 16.2, 15.3. HRMS (ESI, positive) *m/z* $[M+H]^+$ calcd for $C_{43}H_{77}N_2O_6$ 717.5776, found 717.5780.

4.3.5 (20*S*, 24*R*)-Epoxy-3*β*-*N*-butyryl-dammarane-12*β*, 25-diol (**6e**)

Yield, 83%; $[\alpha]_D^{25}$ +15.1 (*c* 1.0, $CHCl_3$); ^{1}H NMR (400 MHz, $CDCl_3$) δ 5.28 (d, *J* = 10.1 Hz, 1H), 3.85 (dd, *J* = 8.9, 6.6 Hz, 1H), 3.67 (ddd, *J* = 12.3, 10.1, 4.1 Hz, 1H), 3.52 (td, *J* = 10.3, 4.6 Hz, 1H), 2.22-2.16 (m, 1H), 2.15 (t, *J* = 7.3 Hz, 2H), 2.08-1.96 (m, 2H), 1.92-1.83 (m, 3H), 1.71-1.62 (m, 5H), 1.59-1.41 (m, 7H), 1.32-0.89 (m, 6H), 1.28 (s, 3H), 1.27 (s, 3H), 1.10 (s, 3H), 0.98 (s, 3H), 0.95 (t, *J* = 7.3 Hz, 3H), 0.90 (s, 3H), 0.86 (s, 3H), 0.84 (s, 3H), 0.76 (s, 3H); ^{13}C NMR (100 MHz, $CDCl_3$) δ 172.4, 86.5, 85.4, 70.9, 70.1, 56.6, 56.1, 52.0, 50.4, 49.4, 47.9, 39.7, 39.4, 39.2, 37.8, 37.0,

34.7, 32.5, 31.2, 31.2, 28.6, 28.4, 27.9, 27.6, 26.1, 25.7, 25.0, 19.4, 18.5, 18.1, 16.3, 16.2, 15.3, 13.7. HRMS (ESI, positive) *m/z* $[M+H]^+$ calcd for $C_{34}H_{60}N_1O_4$ 546.4517, found 546.4530.

4.3.6 (20*S*, 24*R*)-Epoxy-3*β*-*N*-hexanoyl-dammarane-12*β*, 25-diol (**6f**)

Yield, 78%; $[\alpha]_D^{20}$ +17.6 (*c* 1.0, $CHCl_3$); ^{1}H NMR (400 MHz, $CDCl_3$) δ 5.33 (d, *J* = 10.1 Hz, 1H), 3.85 (dd, *J* = 8.7, 6.9 Hz, 1H), 3.67 (ddd, *J* = 12.3, 10.1, 4.12 Hz, 1H), 3.52 (td, *J* = 10.4, 4.7 Hz, 1H), 2.22-2.16 (m, 3H), 2.08-1.83 (m, 5H), 1.71-1.41 (m, 12H), 1.36-0.88 (m, 13H), 1.28 (s, 3H), 1.27 (s, 3H), 1.09 (s, 3H), 0.98 (s, 3H), 0.90 (s, 3H), 0.86 (s,3H), 0.84 (s, 3H), 0.76 (s, 3H); ^{13}C NMR (100 MHz, $CDCl_3$) δ 172.7, 86.5, 85.4, 70.9, 70.1, 56.6, 56.3, 52.0, 50.4, 49.4, 47.9, 39.7, 39.4, 37.8, 37.2, 37.0, 34.7, 32.6, 31.4, 31.2, 31.2, 28.6, 28.4, 27.9, 27.6, 26.1, 25.7, 25.7, 25.0, 22.4, 18.5, 18.1, 16.3, 16.2, 15.3, 13.9. HRMS (ESI, positive) *m/z* $[M+H]^+$ calcd for $C_{36}H_{64}N_1O_4$ 574.4830, found 574.4846.

4.3.7 (20*S*, 24*R*)-Epoxy-3*β*-*N*-octanoyl-dammarane-12*β*, 25-diol (**6g**)

Yield, 90%; $[\alpha]_D^{26}$ +18.7 (*c* 1.0, $CHCl_3$); ^{1}H NMR (400 MHz, $CDCl_3$) δ 5.25 (d, *J* = 10.1 Hz, 1H), 3.85 (dd, *J* = 8.9, 6.6 Hz, 1H), 3.67 (ddd, *J* = 12.3, 10.1, 4.1 Hz, 1H), 3.52 (td, *J* = 10.3, 4.6 Hz, 1H), 2.22-2.16 (m, 1H), 2.17 (t, *J* = 7.8 Hz, 2H), 2.09-1.96 (m, 2H), 1.94-1.83 (m, 3H), 1.71-1.41 (m, 11H), 1.31-0.86 (m, 18H), 1.28 (s, 3H), 1.27 (s, 3H), 1.09 (s, 3H), 0.98 (s, 3H), 0.90 (s, 3H), 0.86 (s, 3H), 0.84 (s, 3H), 0.76 (s, 3H); ^{13}C NMR (100 MHz, $CDCl_3$) δ 172.5, 86.5, 85.4, 70.9, 70.1, 56.6, 56.1, 52.0,

50.4, 49.4, 47.9, 39.7, 39.4, 37.8, 37.3, 37.0, 34.7, 32.6, 31.7, 31.2, 31.2, 29.2, 29.0, 28.6, 28.4, 27.9, 27.6, 26.1, 26.0, 25.7, 25.0, 22.6, 18.5, 18.1, 16.3, 16.2, 15.3, 14.0. HRMS (ESI, positive) *m/z* $[M+H]^+$ calcd for $C_{38}H_{68}N_1O_4$ 602.5143, found 602.5161.

4.3.8 (20*S*, 24*R*)-Epoxy-3*β*-*N*-benzoyl-dammarane-12*β*, 25-diol (**6h**)

Yield, 94%; $[\alpha]_D^{26}$ +19.6 (*c* 1.0, $CHCl_3$); ^{1}H NMR (400 MHz, $CDCl_3$) δ 7.76-7.74 (m, 2H), 7.49 (tt, *J* = 7.3, 1.8 Hz, 1H), 7.45-7.41 (m, 2H), 5.96 (d, *J* = 9.6 Hz, 1H), 3.92-3.83 (m, 2H), 3.54 (td, *J* = 10.5, 4.6 Hz, 1H), 2.20 (td, *J* = 10.1, 3.0 Hz, 1H), 2.09-1.83 (m, 5H), 1.76-1.44 (m, 9H), 1.33-0.90 (m, 7H), 1.28 (s, 3H), 1.27 (s, 3H), 1.10 (s, 3H), 1.00 (s, 3H), 0.95 (s, 3H), 0.92 (s, 3H), 0.87 (s, 3H), 0.86 (s, 3H); ^{13}C NMR (100 MHz, $CDCl_3$) δ 167.1, 135.2, 131.2, 128.5 (2C), 126.8 (2C), 86.5, 85.4, 70.9, 70.1, 56.8, 56.7, 52.0, 50.4, 49.4, 47.9, 39.7, 39.4, 38.1, 37.0, 34.7, 32.6, 31.2, 31.2, 28.6, 28.5, 27.9, 27.6, 26.1, 25.6, 25.0, 18.5, 18.1, 16.4, 16.2, 15.3. HRMS (ESI, positive) *m/z* $[M+H]^+$ calcd for $C_{37}H_{58}N_1O_4$ 580.4360, found 580.4376.

4.3.9 (20*S*, 24*R*)-Epoxy-3*β*-*N*-nicotinoyl-dammarane-12*β*, 25-diol (**6i**)

Yield, 82%; $[\alpha]_D^{25}$ +15.1 (*c* 1.0, $CHCl_3$); ^{1}H NMR (400 MHz, $CDCl_3$) δ 8.94 (d, *J* = 1.4 Hz, 1H), 8.72 (dd, *J* = 4.9, 1.5 Hz, 1H), 8.10 (dt, *J* = 7.8, 1.8 Hz, 1H), 7.39 (dd, *J* = 7.8, 5.0 Hz, 1H), 5.96 (d, *J* = 10.1 Hz, 1H), 3.93-3.83 (m, 2H), 3.54 (td, *J* = 10.5, 4.6 Hz, 1H), 2.20 (td, *J* = 10.1, 3.0 Hz, 1H), 2.09-1.83 (m, 5H), 1.78-1.45 (m, 10H), 1.34-1.90 (m, 6H), 1.28 (s, 3H), 1.27 (s, 3H), 1.10 (s, 3H), 1.00 (s, 3H), 0.95 (s, 3H), 0.92 (s, 3H), 0.89 (s, 3H), 0.87 (s, 3H); ^{13}C NMR (100 MHz, $CDCl_3$) δ 165.1, 152.1,

147.6, 135.1, 130.9, 123.5, 86.5, 85.4, 70.9, 70.1, 57.2, 56.7, 52.0, 50.4, 49.4, 47.9, 39.7, 39.4, 38.1, 37.1, 34.7, 32.6, 31.3, 31.2, 28.6 (2C), 27.9, 27.6, 26.1, 25.6, 25.0, 18.5, 18.2, 16.5, 16.3, 15.4. HRMS (ESI, positive) *m/z* $[M+H]^+$ calcd for $C_{36}H_{57}N_2O_4$ 581.4313, found 581.4332.

4.3.10 (20*S*, 24*R*)-Epoxy-3*β*-*N*-(4-Boc-aminobenzoyl)-dammarane-12*β*, 25-diol (**6j**)

Yield, 75%; $[\alpha]_D^{31}$ +17.2 (*c* 1.0, $CHCl_3$); ^{1}H NMR (400 MHz, $CDCl_3$) δ 7.69 (dd, *J* = 6.9, 1.8 Hz, 2H), 7.43 (d, *J* = 8.7 Hz, 2H), 6.82 (s, 1H), 5.88 (d, *J* = 10.1 Hz, 1H), 3.90-3.83 (m, 2H), 3.53 (td, *J* = 10.5, 4.6 Hz, 1H), 2.20 (td, *J* = 10.1, 3.0 Hz, 1H), 2.09-1.83 (m, 5H), 1.74-0.88 (m, 16H), 1.52 (s, 9H), 1.28 (s, 3H), 1.27 (s, 3H), 1.10 (s, 3H), 0.99 (s, 3H), 0.94 (s, 3H), 0.92 (s, 3H), 0.87 (s, 3H), 0.85 (s, 3H); ^{13}C NMR (100 MHz, $CDCl_3$) δ 166.4, 152.3, 141.3, 129.3, 127.8 (2C), 117.8 (2C), 86.5, 85.4, 81.0, 71.0, 70.1, 56.8, 56.7, 52.0, 50.4, 49.4, 47.9, 39.7, 39.4, 38.2, 37.0, 34.7, 32.6, 31.2, 31.2, 28.6, 28.5, 28.3 (3C), 27.9, 27.6, 26.1, 25.7, 25.0, 18.5, 18.2, 16.5, 16.2, 15.3. HRMS (ESI, positive) *m/z* $[M+H]^+$ calcd for $C_{42}H_{67}N_2O_6$ 695.4994, found 695.5013.

4.3.11 (20*S*, 24*R*)-Epoxy-3*β*-*N*-salicyloyl-dammarane-12*β*, 25-diol (**6k**)

Yield, 88%; $[\alpha]_D^{26}$ +22.5 (*c* 1.0, $CHCl_3$); ^{1}H NMR (400 MHz, $CDCl_3$) δ 12.39 (s, 1H), 7.38 (td, *J* = 7.8, 1.5 Hz, 1H), 7.33 (dd, *J* = 8.2, 1.4 Hz, 1H), 6.98 (dd, *J* = 8.2, 0.9 Hz, 1H), 6.84 (td, *J* = 7.5, 1.2 Hz, 1H), 6.15 (d, *J* = 9.6 Hz, 1H), 3.90-3.83 (m, 2H), 3.54 (td, *J* = 10.3, 4.9 Hz, 1H), 2.20 (td, *J* = 10.1, 3.0 Hz, 1H), 2.08-0.81 (m, 21H), 1.28 (s, 3H), 1.27 (s, 3H), 1.10 (s, 3H), 1.00 (s, 3H), 0.93 (s, 3H), 0.92 (s, 3H),

0.88 (s, 6H); ^{13}C NMR (100 MHz, $CDCl_3$) δ 169.3, 161.5, 134.0, 125.0, 118.6, 118.5, 114.6, 86.5, 85.4, 70.9, 70.1, 56.8, 56.6, 52.0, 50.4, 49.4, 47.9, 39.7, 39.3, 38.0, 37.1, 34.7, 32.6, 31.3, 31.2, 28.6, 28.5, 27.9, 27.6, 26.1, 25.5, 25.0, 18.5, 18.1, 16.4, 16.2, 15.4. HRMS (ESI, positive) *m/z* $[M+H]^+$ calcd for $C_{37}H_{58}N_1O_5$ 596.4310, found 596.4330.

4.3.12 (20*S*, 24*R*)-Epoxy-3*β*-*N*-(2-carboxy benzoyl)-dammarane-12*β*, 25-diol (**6l**)

Yield, 56%; $[\alpha]_D^{27}$ +19.4 (*c* 1.0, MeOH); ^{1}H NMR (400 MHz, CD_3OD) δ 7.88 (d, *J* = 8.2 Hz, 1H), 7.52 (t, *J* = 6.9 Hz, 1H), 7.48 (t, *J* = 6.9 Hz, 1H), 7.41 (d, *J* = 7.3 Hz, 1H), 3.90 (t, *J* = 7.5 Hz, 1H), 3.81 (dd, *J* = 11.9, 4.1 Hz, 1H), 3.51 (td, *J* = 10.5, 4.6 Hz, 1H), 2.24-2.19 (m, 1H), 2.08-0.88 (m, 21H), 1.28 (s, 3H), 1.23 (s, 3H), 1.14 (s, 3H), 1.03 (s, 3H), 1.01 (s, 3H), 0.97 (s, 3H), 0.90 (s, 3H), 0.84 (s, 3H); ^{13}C NMR (100 MHz, CD_3OD) δ 173.3, 173.3, 131.7, 130.9, 130.4, 128.8, 87.9, 86.0, 72.4, 71.9, 58.8, 58.2, 53.3, 51.8, 50.1, 49.8, 41.0, 40.9, 39.7, 38.2, 35.9, 33.7, 32.9, 32.2, 29.6, 29.5, 27.1, 26.8, 26.6, 26.0, 25.6, 19.6, 18.8, 17.1, 16.8, 15.9. HRMS (ESI, positive) *m/z* $[M+H]^+$ calcd for $C_{38}H_{58}N_1O_6$ 624.4259, found 624.4274.

4.3.13 (20*S*, 24*R*)-Epoxy-3*β*-*N*-(2-aminoacetyl)-dammarane-12*β*, 25-diol (**7a**)

Quantitative yield; $[\alpha]_D^{26}$ +21.9 (*c* 1.0, MeOH); ^{1}H NMR (400 MHz, CD_3OD) δ 3.89 (t, *J* = 7.5 Hz, 1H), 3.68 (s, 2H), 3.62 (dd, *J* = 12.6, 3.9 Hz, 1H), 3.49 (td, *J* = 10.5, 4.6 Hz, 1H), 2.20 (td, *J* = 10.9, 3.2 Hz, 1H), 2.07-0.89 (m, 21H), 1.27 (s, 3H), 1.22 (s, 3H), 1.13 (s, 3H), 1.03 (s, 3H), 0.95 (s, 3H), 0.91 (s, 3H), 0.86 (s, 3H), 0.82 (s,

3H); ^{13}C NMR (100 MHz, CD_3OD) δ 166.8, 87.8, 86.0, 72.3, 71.9, 58.8, 58.0, 53.2, 51.8, 50.1, 49.6, 41.5, 41.0, 40.8, 39.3, 38.2, 35.8, 33.7, 32.8, 32.1, 29.6, 29.1, 27.1, 26.8, 26.6, 26.2, 26.0, 19.6, 18.7, 16.9, 16.8, 15.9. HRMS (ESI, positive) *m/z* $[M+H]^+$ calcd for $C_{32}H_{57}N_2O_4$ 533.4313, found 533.4325.

4.3.14 (20*S*, 24*R*)-Epoxy-3*β*-*N*-(4-aminobutyryl)-dammarane-12*β*, 25-diol (**7b**)

Quantitative yield; $[\alpha]_D^{27}$ +23.4 (*c* 1.0, MeOH); ^{1}H NMR (400 MHz, $CDCl_3$) δ 3.89 (t, *J* = 7.5 Hz, 1H), 3.59 (dd, *J* = 12.3, 4.1 Hz, 1H), 3.49 (td, *J* = 10.5, 4.6 Hz, 1H), 2.96 (t, *J* = 7.5 Hz, 2H), 2.37 (t, *J* = 6.9 Hz, 2H), 2.20 (td, *J* = 9.9, 3.7 Hz, 1H), 2.07-0.87 (m, 23H), 1.27 (s, 3H), 1.22 (s, 3H), 1.13 (s, 3H), 1.02 (s, 3H), 0.94 (s, 3H), 0.91 (s, 3H), 0.83 (s, 3H), 0.81 (s, 3H); ^{13}C NMR (100 MHz, $CDCl_3$) δ 174.0, 87.9, 86.0, 72.3, 71.9, 58.2, 58.1, 53.2, 51.8, 50.1, 49.5, 41.0, 40.9, 40.5, 39.4, 38.2, 35.8, 33.9, 33.7, 32.8, 32.2, 29.6, 29.2, 27.1, 26.8, 26.6, 26.2, 26.0, 24.7, 19.7, 18.7, 17.0, 16.8, 15.9. HRMS (ESI, positive) *m/z* $[M+H]^+$ calcd for $C_{34}H_{61}N_2O_4$ 561.4626, found 561.4641.

4.3.15 (20*S*, 24*R*)-Epoxy-3*β*-*N*-(6-aminohexanoyl)-dammarane-12*β*, 25-diol (**7c**)

Quantitative yield; $[\alpha]_D^{22}$ +19.8 (*c* 1.0, MeOH); ^{1}H NMR (400 MHz, CD_3OD) δ 3.89 (t, *J* = 7.3 Hz, 1H), 3.58 (dd, *J* = 12.6, 3.9 Hz, 1H), 3.49 (td, *J* = 10.6, 4.4 Hz, 1H), 2.91 (dd, *J* = 10.3, 4.8 Hz, 2H), 2.26-2.17 (m, 3H), 2.07-0.92 (m, 27H), 1.27 (s, 3H), 1.22 (s, 3H), 1.13 (s, 3H), 1.02 (s, 3H), 0.94 (s, 3H), 0.91 (s, 3H), 0.82 (s, 3H), 0.80 (s, 3H); ^{13}C NMR (100 MHz, CD_3OD) δ175.4, 87.8, 86.0, 72.3, 71.9, 58.1, 58.0,

53.2, 51.8, 50.1, 49.5, 41.0, 40.9, 40.5, 39.4, 38.2, 36.8, 35.8, 33.7, 32.8, 32.2, 29.6, 29.2, 28.3, 27.1, 27.0, 26.7, 26.6 (2C), 26.3, 26.0, 19.7, 18.7, 17.0, 16.8, 15.9. HRMS (ESI, positive) *m/z* $[M+H]^+$ calcd for $C_{36}H_{65}N_2O_4$ 589.4939, found 589.4948.

4.3.16 (20*S*, 24*R*)-Epoxy-3*β*-*N*-(8-aminooctanoyl)-dammarane-12*β*, 25-diol (**7d**)

Quantitative yield; $[\alpha]_D^{27}$ +21.8 (*c* 1.0, MeOH); ^{1}H NMR (400 MHz, CD_3OD) δ 3.89 (t, *J* = 7.3 Hz, 1H), 3.58 (dd, *J* = 12.3, 4.1 Hz, 1H), 3.49 (td, *J* = 10.5, 4.6 Hz, 1H), 2.90 (t, *J* = 7.8 Hz, 2H), 2.30-2.17 (m, 3H), 2.07-0.86 (m, 31H), 1.27 (s, 3H), 1.22 (s, 3H), 1.13 (s, 3H), 1.02 (s, 3H), 0.94 (s, 3H), 0.91 (s, 3H), 0.83 (s, 3H), 0.80 (s, 3H); ^{13}C NMR (100 MHz, CD_3OD) δ 175.8, 87.9, 86.0, 72.4, 71.9, 58.1, 58.0, 53.2, 51.8, 50.1, 49.3, 41.0, 40.9, 40.7, 39.4, 38.2, 37.1, 35.8, 33.7, 32.8, 32.2, 30.0, 29.9, 29.6, 29.2, 28.5, 27.2, 27.1, 27.0, 26.8, 26.6, 26.3, 26.0, 19.7, 18.7, 17.0, 16.8, 15.9. HRMS (ESI, positive) *m/z* $[M+H]^+$ calcd for $C_{38}H_{69}N_2O_4$ 617.5252, found 617.5273.

4.3.17 (20*S*, 24*R*)-Epoxy-3*β*-*N*-(4-aminobenzoyl)-dammarane-12*β*, 25-diol (**7e**)

Quantitative yield; $[\alpha]_D^{26}$ +32.4 (*c* 1.0, $CHCl_3$: MeOH = 1:4); ^{1}H NMR (400 MHz, CD_3OD / $CDCl_3$ = 4/1) δ 7.74 (d, *J* = 8.2 Hz, 2H), 7.04 (d, *J* = 8.7 Hz, 2H), 3.89 (t, *J* = 7.5 Hz, 1H), 3.82 (dd, *J* = 12.1, 3.9 Hz, 1H), 3.51 (td, *J* = 10.5, 4.6 Hz, 1H), 2.20 (td, *J* = 9.9, 3.0 Hz, 1H), 2.07-0.91 (m, 21H), 1.27 (s, 3H), 1.23 (s, 3H), 1.12 (s, 3H), 1.03 (s, 3H), 0.95 (s, 3H), 0.93 (s, 3H), 0.88 (s, 6H); ^{13}C NMR (100 MHz, CD_3OD / $CDCl_3$ = 4/1) δ 169.3, 143.8, 130.2, 130.0 (2C), 119.2 (2C), 87.7, 85.9, 72.2, 71.7, 58.4, 57.9, 53.1, 51.6, 49.9, 49.5, 40.8 (2C), 39.7, 38.1, 35.7, 33.6, 32.6, 32.0, 29.5, 29.2, 27.3,

26.9, 26.5, 25.9, 25.8, 19.5, 18.7, 17.1, 16.8, 15.9. HRMS (ESI, positive) *m/z* $[M+H]^+$ calcd for $C_{37}H_{59}N_2O_4$ 595.4469, found 595.4483.

4.3.18 (20*S*, 24*S*)-Epoxy-3*β*-*N*-(2-Boc-aminoacetyl)-dammarane-12*β*, 25-diol (**11a**)

Yield, 90%; $[\alpha]_D^{24}$ +7.8 (*c* 1.0, $CHCl_3$); ^1H NMR (400 MHz, $CDCl_3$) δ 6.06 (d, *J* = 9.6 Hz, 1H), 5.19 (s, 1H), 3.88 (dd, *J* = 10.7, 5.3 Hz, 1H), 3.78 (dd, *J* = 16.5, 5.9 Hz, 1H), 3.72 (dd, *J* = 16.5, 5.9 Hz, 1H), 3.68-3.61 (m, 1H), 3.53 (td, *J* = 10.3, 4.7 Hz, 1H), 2.25 (td, *J* = 10.3, 4.4 Hz, 1H), 2.10-0.77 (m, 21H), 1.45 (s, 9H), 1.28 (s, 3H), 1.23 (s, 3H), 1.10 (s, 3H), 1.01 (s, 3H), 0.91 (s, 3H), 0.88 (s, 3H), 0.86 (s, 3H), 0.77 (s, 3H); ^{13}C NMR (100 MHz, $CDCl_3$) δ 168.9, 156.2, 87.3, 87.1, 80.2, 70.5, 70.0, 56.6, 56.6, 52.1, 50.1, 48.9, 48.8, 44.9, 39.7, 39.3, 37.9, 37.0, 34.6, 32.1, 31.6, 31.6, 28.8, 28.5, 28.3, 28.3 (3C), 28.0, 25.5, 25.0, 24.2, 18.5, 17.7, 16.2 (2C), 15.4. HRMS (ESI, positive) *m/z* $[M+H]^+$ calcd for $C_{37}H_{65}N_2O_6$ 633.4837, found 633.4847.

4.3.19 (20*S*, 24*S*)-Epoxy-3*β*-*N*-(4-Boc-aminobutyryl)-dammarane-12*β*, 25-diol (**11b**)

Yield, 90%; $[\alpha]_D^{21}$ +6.9 (*c* 1.0, $CHCl_3$); ^1H NMR (400 MHz, $CDCl_3$) δ 4.64 (s, 1H), 4.49 (dd, *J* = 11.0, 5.5 Hz, 1H), 3.88 (dd, *J* = 10.7, 5.3 Hz, 1H), 3.53 (td, *J* = 10.2, 4.7 Hz, 1H), 3.16 (dd, *J* = 12.3, 6.4 Hz, 2H), 2.34 (t, *J* = 7.5 Hz, 2H), 2.25 (td, *J* = 10.3, 4.4 Hz, 1H), 2.12-0.88 (m, 23H), 1.43 (s, 9H), 1.28 (s, 4H), 1.23 (s, 3H), 1.10 (s, 3H), 1.02 (s, 3H), 0.91 (s, 6H), 0.86 (s, 3H), 0.84 (s, 3H) ; ^{13}C NMR (100 MHz, $CDCl_3$) δ 173.0, 155.9, 87.4, 87.1, 80.9, 79.2, 70.5, 70.0, 56.0, 52.1, 50.1, 48.9, 48.8, 40.0, 39.7, 38.5, 37.9, 37.1, 34.7, 32.2, 32.0, 31.6, 31.6, 28.8, 28.5, 28.4 (3C), 28.0 (2C), 25.3,

25.0, 24.2, 23.7, 18.2, 17.7, 16.5, 16.3, 15.4. HRMS (ESI, positive) *m/z* $[M+H]^+$ calcd for $C_{39}H_{68}N_1O_7$ 662.4990, found 662.5003.

4.3.20 (20*S*, 24*S*)-Epoxy-3*β*-*N*-(6-Boc-aminohexanoyl)-dammarane-12*β*, 25-diol (**11c**)

Yield, 90%; $[\alpha]_D^{24}$ +5.8 (*c* 1.0, $CHCl_3$); ^{1}H NMR (400 MHz, $CDCl_3$) δ 5.92 (s, 1H), 5.40 (d, *J* = 9.6 Hz, 1H), 4.67 (s, 1H), 3.94 (dd, *J* = 10.7, 5.3 Hz, 1H), 3.74 (ddd, *J* = 12.3, 10.1, 4.6 Hz, 1H), 3.61 (td, *J* = 10.4, 4.7 Hz, 1H), 3.28-2.99 (m, 2H), 2.32 (td, *J* = 10.3, 4.3 Hz, 1H), 2.25 (t, *J* = 7.5 Hz, 2H), 2.21-1.88 (m, 7H), 1.88-1.68 (m, 5H), 1.67-1.53 (m, 8H), 1.50 (s, 9H), 1.34 (s, 3H), 1.30 (s, 3H), 1.17 (s, 3H), 1.08 (s, 3H), 0.98 (s, 3H), 0.94 (s, 3H), 0.93 (s, 3H), 0.83 (s, 3H); ^{13}C NMR (100 MHz, $CDCl_3$) δ 172.4, 156.0, 87.3, 87.1, 79.0, 70.5, 70.1, 56.5, 56.2, 52.1, 50.1, 48.8, 48.7, 40.3, 39.6, 39.3, 37.8, 37.0 (2C), 34.6, 32.1, 31.6, 31.5, 28.8, 28.5, 28.4 (5C), 27.9, 26.3, 25.7, 25.5, 25.1, 24.1, 18.5, 17.7, 16.4, 16.1, 15.4. HRMS (ESI, positive) *m/z* $[M+H]^+$ calcd for $C_{41}H_{73}N_2O_6$ 689.5463, found 689.5472.

4.3.21 (20*S*, 24*S*)-Epoxy-3*β*-*N*-(8-Boc-aminooctanoyl)-dammarane-12*β*, 25-diol (**11d**)

Yield, 100%; $[\alpha]_D^{24}$ +5.9 (*c* 1.0, $CHCl_3$); ^{1}H NMR (400 MHz, $CDCl_3$) δ 5.31 (d, *J* = 10.1 Hz, 1H), 4.54 (s, 1H), 3.88 (dd, *J* = 11.0, 5.5 Hz, 1H), 3.67 (ddd, *J* = 12.3, 10.1, 4.57 Hz, 1H), 3.53 (td, *J* = 10.3, 4.7 Hz, 1H), 3.12-3.07 (m, 2H), 2.25 (td, *J* = 10.3, 4.0 Hz, 1H), 2.17 (t, *J* = 7.5 Hz, 2H), 2.10-0.72 (m, 31H), 1.44 (s, 9H), 1.28 (s, 3H), 1.23 (s, 3H), 1.10 (s, 3H), 1.01 (s, 3H), 0.92 (s, 3H), 0.87 (s, 3H), 0.87 (s, 3H), 0.77 (s,

3H); ^{13}C NMR (100 MHz, $CDCl_3$) δ 172.5, 156.0, 87.3, 87.1, 79.0, 70.5, 70.0, 56.6, 56.2, 52.1, 50.1, 48.9, 48.8, 40.4, 39.7, 39.3, 37.8, 37.1, 37.0, 34.6, 32.1, 31.6, 31.5, 29.9, 29.1, 28.9, 28.8, 28.5, 28.4 (4C), 27.9, 26.5, 25.8, 25.7, 25.0, 24.2, 18.5, 17.7, 16.4, 16.1, 15.4. HRMS (ESI, positive) *m/z* $[M+H]^+$ calcd for $C_{43}H_{77}N_2O_6$ 717.5776, found 717.5765.

4.3.22 (20*S*, 24*S*)-Epoxy-3*β*-*N*-hexanoyl-dammarane-12*β*, 25-diol (**11e**)

Yield： 83%; $[\alpha]_D^{25}$ +7.3 (*c* 1.0, $CHCl_3$); ^{1}H NMR (400 MHz, $CDCl_3$) δ 5.72 (s, 1H), 5.25 (d, *J* = 10.1 Hz, 1H), 3.87 (dd, *J* = 10.5, 5.5 Hz, 1H), 3.68 (ddd, *J* = 12.3, 10.1, 4.6 Hz, 1H), 3.53 (td, *J* = 10.4, 4.7 Hz, 1H), 2.25 (td, *J* = 10.4, 4.3 Hz, 1H), 2.17 (t, *J* = 7.5 Hz, 2H), 2.10-0.61 (m, 30H), 1.28 (s, 3H), 1.23 (s, 3H), 1.10 (s, 3H), 1.01 (s, 3H), 0.92 (s, 3H), 0.87 (s, 6H), 0.76 (s, 3H);; ^{13}C NMR (100 MHz, $CDCl_3$) δ 172.5, 87.3, 87.1, 70.5, 70.0, 56.6, 56.1, 52.1, 50.1, 48.9, 48.8, 39.7, 39.3, 37.8, 37.3, 37.0, 34.6, 32.1, 31.6 (2C), 31.4, 28.8, 28.5, 28.4, 28.0, 25.7, 25.6, 25.0, 24.2, 22.4, 18.5, 17.7, 16.4, 16.2, 15.4, 13.9. HRMS (ESI, positive) *m/z* $[M+H]^+$ calcd for $C_{36}H_{64}N_1O_4$ 574.4830, found 574.4840.

4.3.23 (20*S*, 24*S*)-Epoxy-3*β*-*N*-benzoyl-dammarane-12*β*, 25-diol (**11f**)

Yield, 94%; $[\alpha]_D^{27}$ +12.3 (*c* 1.0, $CHCl_3$); ^{1}H NMR (400 MHz, $CDCl_3$) δ 7.77-7.74 (m, 2H), 7.52-7.41 (m, 3H), 5.94 (d, *J* = 10.1 Hz, 1H), 5.74 (s, 1H), 3.93-3.86 (m, 2H), 3.55 (td, *J* = 10.3, 4.9 Hz, 1H), 2.27 (td, *J* = 10.3, 4.3 Hz, 1H), 2.11-1.46 (m, 16H), 1.33-0.87 (m, 5H), 1.28 (s, 3H), 1.23 (s, 3H), 1.11 (s, 3H), 1.03 (s, 3H), 0.96 (s, 3H),

0.94 (s, 3H), 0.91 (s, 3H), 0.87 (s, 3H); ^{13}C NMR (100 MHz, $CDCl_3$) δ 167.0, 135.3, 131.2, 128.6 (2C), 126.8 (2C), 87.3, 87.1, 70.5, 70.0, 56.8, 56.7, 52.2, 50.1, 48.9, 48.8, 39.7, 39.4, 38.2, 37.1, 34.7, 32.2, 31.6, 31.6, 28.9, 28.5 (2C), 28.0, 25.7, 25.0, 24.2, 18.6, 17.7, 16.5, 16.2, 15.4. HRMS (ESI, positive) *m/z* $[M+H]^+$ calcd for $C_{37}H_{58}N_1O_4$ 580.4360, found 580.4377.

4.3.24 (20*S*, 24*S*)-Epoxy-3*β*-*N*-nicotinoyl-dammarane-12*β*, 25-diol (**11g**)

Yield, 94%; $[\alpha]_D^{27}$ +11.2 (*c* 1.0, $CHCl_3$); ^{1}H NMR (400 MHz, $CDCl_3$) δ 8.96 (d, *J* = 0.9 Hz, 1H), 8.72 (dd, *J* = 5.0, 0.9 Hz, 1H), 8.12 (dt, *J* = 8.2, 1.8 Hz, 1H), 7.40 (dd, *J* = 7.8, 4.6 Hz, 1H), 6.05 (d, *J* = 10.1 Hz, 1H), 5.75 (s, 1H), 3.94-3.86 (m, 2H), 3.55 (td, *J* = 10.3, 4.7 Hz, 1H), 2.26 (td, *J* = 10.3, 4.3 Hz, 1H), 2.11-0.96 (m, 21H), 1.28 (s, 3H), 1.23 (s, 3H), 1.11 (s, 3H), 1.03 (s, 3H), 0.96 (s, 3H), 0.94 (s, 3H), 0.92 (s, 3H), 0.88 (s, 3H); ^{13}C NMR (100 MHz, $CDCl_3$) δ 165.0, 151.9, 147.4, 135.3, 130.9, 123.6, 87.3, 87.1, 70.4, 70.0, 57.2, 56.6, 52.1, 50.1, 48.9, 48.8, 39.7, 39.3, 38.1, 37.1, 34.6, 32.2, 31.6 (2C), 28.8, 28.5, 28.5, 27.9, 25.6, 25.0, 24.2, 18.5, 17.7, 16.5, 16.2, 15.4. HRMS (ESI, positive) *m/z* $[M+H]^+$ calcd for $C_{36}H_{57}N_2O_4$ 581.4313, found 581.4327.

4.3.25 (20*S*, 24*S*)-Epoxy-3*β*-*N*-salicyloyl-dammarane-12*β*, 25-diol (**11h**)

Yield, 92%; $[\alpha]_D^{26}$ +18.4 (*c* 1.0, $CHCl_3$); ^{1}H NMR (400 MHz, $CDCl_3$) δ 12.39 (s, 1H), 7.39 (t, *J* = 8.5 Hz, 1H), 7.33 (d, *J* = 7.7 Hz, 1H), 6.99 (d, *J* = 8.2 Hz, 1H), 6.85 (t, *J* = 7.4 Hz, 1H), 6.16 (d, *J* = 9.9 Hz, 1H), 3.91-3.85 (m, 2H), 3.56 (td, *J* = 10.2, 4.8 Hz, 1H), 2.27 (td, *J* = 10.2, 4.2 Hz, 1H), 2.11-0.89 (m, 21H), 1.28 (s, 3H), 1.24 (s, 3H),

1.11 (s, 3H), 1.03 (s, 3H), 0.94 (s, 3H), 0.93 (s, 3H), 0.92 (s, 3H), 0.89 (s, 3H); ^{13}C NMR (100 MHz, $CDCl_3$) δ 169.3, 161.5, 134.0, 125.0, 118.7, 118.5, 114.6, 87.4, 87.1, 70.5, 70.0, 56.7, 56.6, 52.1, 50.1, 48.9, 48.8, 39.7, 39.3, 38.0, 37.1, 34.6, 32.2, 31.6, 31.6, 28.9, 28.5, 28.5, 28.0, 25.5, 25.1, 24.2, 18.5, 17.7, 16.4, 16.2, 15.4. HRMS (ESI, positive) *m/z* $[M+H]^+$ calcd for $C_{37}H_{58}N_1O_5$ 596.4310, found 596.4320.

4.3.26 (20*S*, 24*S*)-Epoxy-3*β*-*N*-(2-aminoacetyl)-dammarane-12*β*, 25-diol (**12a**)

Quantitative yield; $[\alpha]_D^{26}$ +8.8 (*c* 1.0, MeOH); ^{1}H NMR (400 MHz, CD_3OD) δ 3.81 (dd, *J* = 10.5, 5.0 Hz, 1H), 3.70 (dd, *J* = 17.4, 1.4 Hz, 1H), 3.67 (dd, *J* = 17.4, 1.4 Hz, 1H), 3.63 (dd, *J* = 12.6, 4.3 Hz, 1H), 3.51 (td, *J* = 10.4, 4.7 Hz, 1H), 2.23 (td, *J* = 10.2, 3.7 Hz, 1H), 2.04-0.84 (m, 21H), 1.26 (s, 3H), 1.17 (s, 3H), 1.10 (s, 3H), 1.05 (s, 3H), 0.95 (s, 3H), 0.94 (s, 3H), 0.87 (s, 3H), 0.82 (s, 3H); ^{13}C NMR (100 MHz, CD_3OD) δ 166.8, 89.0, 88.5, 72.1, 71.3, 58.8, 58.0, 53.3, 51.5, 50.2, 49.8, 41.5, 41.0, 40.8, 39.3, 38.2, 35.8, 33.4, 32.8, 32.7, 29.4, 29.1 (2C), 26.5, 26.2 (2C), 26.1, 19.7, 18.3, 16.9, 16.8, 15.9. HRMS (ESI, positive) *m/z* $[M+H]^+$ calcd for $C_{32}H_{57}N_2O_4$ 533.4313, found 533.4321.

4.3.27 (20*S*, 24*S*)-Epoxy-3*β*-*N*-(4-aminobutyryl)-dammarane-12*β*, 25-diol (**12b**)

Quantitative yield; $[\alpha]_D^{25}$ -0.6 (*c* 1.0, $CHCl_3$: MeOH = 1:4); ^{1}H NMR (400 MHz, CD_3OD / $CDCl_3$ = 4/1) δ 3.80 (dd, *J* = 10.7, 4.8 Hz, 1H), 3.58 (dd, *J* = 12.6, 4.3 Hz, 1H), 3.49 (td, *J* = 10.3, 4.6 Hz, 1H), 2.93 (t, *J* = 7.3 Hz, 2H), 2.36 (t, *J* = 6.9 Hz, 2H), 2.22 (td, *J* = 10.2, 3.7 Hz, 1H), 2.06-0.84 (m, 23H), 1.25 (s, 3H), 1.17 (s, 3H), 1.10 (s,

3H), 1.03 (s, 3H), 0.93 (s, 3H), 0.90 (s, 3H), 0.82 (s, 3H), 0.79 (s, 3H); ^{13}C NMR (100 MHz, CD_3OD / $CDCl_3$ = 4/1) δ 173.6, 88.5, 88.1, 71.7, 71.1, 57.9, 57.6, 53.0, 51.2, 49.8, 49.8, 40.6, 40.5, 40.1, 39.0, 37.9, 37.0, 35.5, 33.1, 32.5, 32.3, 29.1, 29.0, 26.5, 25.9, 25. 9, 25.7, 24.3, 19.3, 18.3, 16.8, 16.7, 15.9. HRMS (ESI, positive) *m/z* $[M+H]^+$ calcd for $C_{34}H_{61}N_2O_4$ 561.4626, found 561.4632.

4.3.28 (20*S*, 24*S*)-Epoxy-3*β*-*N*-(6-aminohexanoyl)-dammarane-12*β*, 25-diol (**12c**)

Quantitative yield; $[\alpha]_D^{26}$ +7.4 (*c* 1.0, MeOH); ^{1}H NMR (400 MHz, CD_3OD / $CDCl_3$ = 4/1) δ 3.80 (dd, *J* = 10.5, 5.0 Hz, 1H), 3.58 (dd, *J* = 12.3, 4.1 Hz, 1H), 3.50 (td, *J* = 10.4, 4.7 Hz, 1H), 2.89 (t, *J* = 7.8 Hz, 2H), 2.31-2.19 (m, 3H), 2.03-0.77 (m, 27H), 1.26 (s, 3H), 1.17 (s, 3H), 1.10 (s, 3H), 1.03 (s, 3H), 0.94 (s, 3H), 0.91 (s, 3H), 0.82 (s, 3H), 0.79 (s, 3H); ^{13}C NMR (100 MHz, CD_3OD / $CDCl_3$ = 4/1) δ 175.1, 88.7, 88.2, 71.8, 71.1, 57.8, 57.8, 53.1, 51.3, 49.9, 49.5, 40.7, 40.7, 40.3, 39.2, 38.0, 36.6, 35.6, 33.2, 32.6, 32.4, 29.2, 29.1, 29.1, 28.0, 26.8, 26.5, 26.3, 26.1, 26.0, 25.9, 19.5, 18.3, 16.9, 16.8, 15.9. HRMS (ESI, positive) *m/z* $[M+H]^+$ calcd for $C_{36}H_{65}N_2O_4$ 589.4939, found 589.4945.

4.3.29 (20*S*, 24*S*)-Epoxy-3*β*-*N*-(8-aminooctanoyl)-dammarane-12*β*, 25-diol (**12d**)

Quantitative yield; $[\alpha]_D^{25}$ +21.4 (*c* 1.0, MeOH); ^{1}H NMR (400 MHz, CD_3OD) δ 3.80 (dd, *J* = 10.3, 4.8 Hz, 1H), 3.58 (dd, *J* = 12.3, 4.1 Hz, 1H), 3.51 (td, *J* = 10.3, 4.6 Hz, 1H), 2.90 (t, *J* = 7.8 Hz, 2H), 2.27-2.15 (m, 3H), 2.04-0.77 (m, 31H), 1.26 (s, 3H), 1.17 (s, 3H), 1.10 (s, 3H), 1.05 (s, 3H), 0.95 (s, 3H), 0.93 (s, 3H), 0.83 (s, 3H), 0.80 (s,

3H); ^{13}C NMR (100 MHz, CD_3OD) δ 175.8, 88.9, 88.5, 72.1, 71.3, 58.1, 58.0, 53.3, 51.5, 50.2, 49.8, 40.9, 40.9, 40.7, 39.4, 38.2, 37.1, 35.8, 33.4, 32.8, 32.6, 30.0, 29.9, 29.4, 29.2, 29.1, 28.5, 27.2, 27.1, 26.5, 26.3, 26.2, 26.1, 19.7, 18.3, 17.0, 16.8, 15.9. HRMS (ESI, positive) *m/z* $[M+H]^+$ calcd for $C_{38}H_{69}N_2O_4$ 617.5252, found 617.5262.

4.4. Cell culture

KBV cells were obtained from Dr. Xiaoguang Chen (Institute Materia Medica, Chinese Academy of Medical Sciences) and cultured in our lab [23]. The cells were cultured in DMEM media supplemented with 10% fetal calf serum, penicillin (100 U/mL), and streptomycin (100 mg/mL), and incubated at 37 °C in a humidified atmosphere containing 5% CO_2. All cells were harvested during the exponential growth phase. In addition, 10 nM paclitaxel was added to the medium to maintain resistance toward the drug.

4.5. Cytotoxicity and MDR reversal assay

The MTT assay was used to determine cell viability as per our previous protocol [29]. In short, cells were seeded into 96-well plates and treated with test compounds the next day. After being incubated for 72 h, cells were treated with MTT solution for 2 h. After the supernatant was discarded, the residue was dissolved in 150 μL of DMSO with gentle shaking for 5 min. The absorbance at 570 nm was measured and used to calculate the cell survival rate.

4.6. Intracellular Rhodamine123 accumulation assay

The effect of **6c** on the Rhodamine123 accumulation was measured by flow cytometry analysis following our previous protocol [23]. Briefly, KBV cells were treated with or without **6c** for 2 h at the indicated concentrations, and then the cells were incubated with 10 μM Rhodamine123 for 30 min. Subsequently, the cells were harvested and washed three times with PBS buffer prior to analysis by flow cytometry. The mean fluorescence intensity was then automatically calculated from the fluorescence intensity of 10,000 cells by a flow cytometry machine (BD, C6, USA).

4.7. Cell cycle distribution analysis

A flow cytometry assay was used to analyze the cell cycle distribution as previously reported [29]. Briefly, the cells were cultured for 24 h in a 6-well plate, then the test compound was added to the culture medium. After treatment for the indicated time, the cells were harvested and fixed in ethanol solution (70%) overnight at –20 °C, and then washed with PBS and stained with PI solution (20 mg/mL PI and 20 mg/mL RNaseA in PBS) for 30 min. The cell fluorescence was measured using a flow cytometry machine (BD, C6, USA) and the cell cycle distribution was analyzed.

4.8 ATPase activity assay

The Pgp-Glo™ assay kit (Promega, USA) was used to detect the effect of **6c** on the ATPase activity following our published protocol [23]. Briefly, the diluted Pgp protein was added into the wells containing **6c**, or the positive control, verapamil. After

incubation at 37 °C for 5 min, MgATP were added and mixed, and then incubated for 40 min at 37 °C. The reactions were stopped and the luminescence initiated by adding ATP Detection Reagent. Solutions were mixed, and then plates were incubated at rt for 20 min. Luminescence was read using a SpectraMax M5 multifunctional microplate reader (Molecular Devices, USA).

4.9 Xenograft Studies

Nude mice (6–8 weeks old, BALB/c, male) were used to develop the xenograft tumor model following our published protocol [30]. Briefly, KBV cells (5×10^6) were implanted into the backs of the mice by subcutaneous injection. When the tumor reached 100–200 mm^3, the mice were randomly divided into four groups (four animals per group): control group; paclitaxel (30 mg/kg); **6c** (10 mg/kg); paclitaxel (30 mg/kg) and **6c** (10 mg/kg). Treatment was administered once every 3 days via intraperitoneal injection for paclitaxel, and every day via gavage for **6c**. The tumor growth was measured every 3 days during the treatment. At the end of the treatment, mice were sacrificed and the tumors were removed and weighed. The use of animals was approved by the Animal Experimentation Ethics Committee of Yantai University (protocol number 20180407) in accordance with the guidelines for ethical conduct in the care and use of animals.

4.10 Molecular modeling

The possible binding mode of the compounds and the homology receptor of human

Pgp [27] was predicted using the Surflex-Dock module in SYBYL-X2.1.1 [31]. The binding site of the homology receptor was recognized as the area around the key residues in contact with QZ-RRR, QZ-SSS, and verapamil, as established by Li [27]. Default settings for compound–protein dockings were used throughout the simulations.

4.11 Statistical analysis

Data were presented as mean ± SD. The statistical significance of differences between groups was evaluated by the Student's *t*-test and indicated with **: $p < 0.01$, *: $p < 0.05$.

Competing interest

The authors declare no competing financial interest.

Acknowledgment

This study was supported by National Natural Science Foundation of China (No. 21502164 and 81728020), Promotive Research Fund for Excellent Young and Middle-age Scientists of Shandong Province (No. BS2015YY039), Key Research Project of Shandong Province (2017GSF18177), Natural Science Foundation of Shandong Province (ZR2018LH025), Key Research Project of Yantai City (No. 2018ZHGY085).

References

[1]. G. Szakács, J.K. Paterson, J.A. Ludwig, C. Booth-Genthe, M.M. Gottesman, Targeting multidrug resistance in cancer. Nat. Rev. Drug Discovery 5 (2006) 219.

[2]. B. Sarkadi, L. Homolya, G. Szakacs, A. Varadi, Human multidrug resistance ABCB and ABCG transporters: participation in a chemoimmunity defense system. Physiol. Rev. 86 (2006) 1179-236.

[3]. N.A. Colabufo, F. Berardi, M. Cantore, M. Contino, C. Inglese, M. Niso, R. Perrone, Perspectives of P-glycoprotein modulating agents in oncology and neurodegenerative diseases: pharmaceutical, biological, and diagnostic potentials. J. Med. Chem. 53 (2010) 1883-97.

[4]. R. Hu, J. Gao, R. Rozimamat, H.A. Aisa, Jatrophane diterpenoids from Euphorbia sororia as potent modulators against P-glycoprotein-based multidrug resistance. Eur. J. Med. Chem. 146 (2018) 157-170.

[5]. R.J. Kathawala, P. Gupta, C.R. Ashby, Z.-S. Chen, The modulation of ABC transporter-mediated multidrug resistance in cancer: A review of the past decade. Drug Resist. Updat. 18 (2015) 1-17.

[6]. A. Paterna, A. Kincses, G. Spengler, S. Mulhovo, J. Molnar, M.J.U. Ferreira, Dregamine and tabernaemontanine derivatives as ABCB1 modulators on resistant cancer cells. Eur. J. Med. Chem. 128 (2017) 247-257.

[7]. A.S. Attele, J.A. Wu, C.S. Yuan, Ginseng pharmacology: multiple constituents and multiple actions. Biochem. Pharmacol. 58 (1999) 1685-93.

[8]. C. Liu, Q. Gong, T. Chen, J. Lv, Z.P. Feng, P.J. Liu, Z.Y. Deng, Treatment with 20(S)-ginsenoside Rg3 reverses multidrug resistance in A549/DDP xenograft tumors. Oncology Letters 15 (2018) 4376-4382.

[9]. J.W. Zhang, F. Zhou, X.L. Wu, X.X. Zhang, Y.C. Chen, B.S. Zha, F. Niu, M. Lu, G. Hao, Y. Sun, J.G. Sun, Y. Peng, G.J. Wang, Cellular pharmacokinetic mechanisms of adriamycin resistance and its modulation by 20(S)-ginsenoside Rh2 in MCF-7/Adr cells. Br. J. Pharmacol. 165 (2012) 120-134.

[10]. S.W. Kim, H.Y. Kwon, D.W. Chi, J.H. Shim, J.D. Park, Y.H. Lee, S. Pyo, D.K. Rhee, Reversal of P-glycoprotein-mediated multidrug resistance by ginsenoside Rg3. Biochem. Pharmacol. 65 (2003) 75-82.

[11]. J.H. Liu, X. Wang, P. Liu, R.X. Deng, M. Lei, W.T. Chen, L.H. Hu, 20(S)-Protopanaxadiol (PPD) analogues chemosensitize multidrug-resistant cancer cells to clinical anticancer drugs. Bioorg. Med. Chem. 21 (2013) 4279-4287.

[12]. Y. Zhao, L. Bu, H. Yan, W. Jia, 20S-protopanaxadiol inhibits P-glycoprotein in multidrug resistant cancer cells. Planta Med. 75 (2009) 1124-8.

[13]. B. Han, Q.G. Meng, Q.A. Li, J.F. Zhang, Y. Bi, N.C. Jiang, Effect of 20(S)-protopanaxatriol and its epimeric derivatives on myocardial injury induced by isoproterenol. Arzneimittelforschung-Drug Research 61 (2011) 148-152.

[14]. Y. Bi, T. Wang, Q.G. Meng, J.F. Zhang, L. Wang, Q. Li, F.L. Zhao, H.J. Sun, Synthesis and Myocardial Ischemia Protective Effect of Ocotillol-Type Derivatives. Rec. Nat. Prod. 6 (2012) 242-254.

[15]. G.Q. Yang, Y.T. Yang, Q. Yang, Y. Li, Y.T. Jiang, F.H. Fu, H.B. Wang, Novel Fluorescent Pyxinol-Based Probes: Design, Synthesis and Biological Evaluation. Chin. J. Org. Chem. 37 (2017) 2109-2114.

[16]. Y. Bi, C. Ma, Z.W. Zhou, T.T. Zhang, H.Y. Zhang, X.C. Zhang, J. Lu, Q.G. Meng, P.J. Lewis, J.Y. Xu, Synthesis and Antibacterial Evaluation of Novel Hydrophilic Ocotillol-Type Triterpenoid

Derivatives from 20(S)-Protopanaxadiol. Rec. Nat. Prod. 9 (2015) 356-368.

[17]. Y. Bi, J. Yang, C. Ma, Z.Y. Liu, T.T. Zhang, X.C. Zhang, J. Lu, Q.G. Meng, Design, synthesis and in vitro NO-releasing activities of ocotillol-type furoxans. Pharmazie 70 (2015) 213-218.

[18]. J. Liu, Y.R. Xu, J.J. Yang, W.Z. Wang, J.Q. Zhang, R.M. Zhang, Q.G. Meng, Discovery, semisynthesis, biological activities, and metabolism of ocotillol-type saponins. Journal of Ginseng Research 41 (2017) 373-378.

[19].Z.W. Zhou, C. Ma, H.Y. Zhang, Y. Bi, X. Chen, H. Tian, X.N. Xie, Q.G. Meng, P.J. Lewis, J.Y. Xu, Synthesis and biological evaluation of novel ocotillol-type triterpenoid derivatives as antibacterial agents. Eur. J. Med. Chem. 68 (2013) 444-53.

[20].Y. Bi, X. Yang, T.T. Zhang, Z.Y. Liu, X.C. Zhang, J. Lu, K.G. Cheng, J.Y. Xu, H.B. Wang, G.Y. Lv, P.J. Lewis, Q.G. Meng, C. Ma, Design, synthesis, nitric oxide release and antibacterial evaluation of novel nitrated ocotillol-type derivatives. Eur. J. Med. Chem. 101 (2015) 71-80.

[21]. L. Li, X.Y. Chen, D. Li, D.F. Zhong, Identification of 20(S)-protopanaxadiol metabolites in human liver microsomes and human hepatocytes. Drug Metab. Dispos. 39 (2011) 472-83.

[22]. W.Y. Wang, Y.Y. Ni, L. Wang, X. Che, W.H. Liu, Q.G. Meng, Stereoselective oxidation metabolism of 20(S)-protopanaxatriol in human liver microsomes and in rats. Xenobiotica 45 (2015) 385-395.

[23]. Y.T. Yang, D.K. Guan, L. Lei, J. Lu, J.Q. Liu, G.Q. Yang, C.H. Yan, R. Zhai, J.W. Tian, Y. Bi, F.H. Fu, H.B. Wang, H6, a novel hederagenin derivative, reverses multidrug resistance in vitro and in vivo. Toxicol. Appl. Pharmacol. 341 (2018) 98-105.

[24]. G.Q. Yang, Y. Li, Q. Yang, X. Yue, L. Yao, Y.T. Jiang, Simple and Efficient Synthesis of Pseudoginsenoside HQ. Chin. J. Org. Chem. 37 (2017) 1530-1536.

[25]. Y.K. Zhang, H.Y. Zhang, G.N. Zhang, Y.J. Wang, R.J. Kathawala, R. Si, B.A. Patel, J.Y. Xu, Z.S. Chen, Semi-synthetic ocotillol analogues as selective ABCB1-mediated drug resistance reversal agents. Oncotarget 6 (2015) 24277-24290.

[26].P.B. Schiff, S.B. Horwitz, Taxol stabilizes microtubules in mouse fibroblast cells. Proc. Natl. Acad. Sci. U. S. A. 77 (1980) 1561-1565.

[27]. J. Li, K.F. Jaimes, S.G. Aller, Refined structures of mouse P-glycoprotein. Protein Sci 23 (2014) 34-46.

[28]. W.Y. Wang, X.M. Wu, L. Wang, Q.G. Meng, W.H. Liu, Stereoselective Property of 20(S)-Protopanaxadiol Ocotillol Type Epimers Affects Its Absorption and Also the Inhibition of P-Glycoprotein. PLoS One 9 (2014).

[29]. G.Y. Lv, D.J. Sun, J.W. Zhang, X.X. Xie, X.Q. Wu, W.S. Fang, J.W. Tian, C.H. Yan, H.B. Wang, F.H. Fu, Lx2-32c, a novel semi-synthetic taxane, exerts antitumor activity against prostate cancer cells in vitro and in vivo. Acta Pharmaceutica Sinica B 7 (2017) 52-58.

[30]. Y.T. Ma, Y.T. Yang, P. Cai, D.Y. Sun, P.A. Sanchez-Murcia, X.Y. Zhang, W.Q. Jia, L. Lei, M.Q. Guo, F. Gago, H.B. Wang, W.S. Fang, A Series of Enthalpically Optimized Docetaxel Analogues Exhibiting Enhanced Antitumor Activity and Water Solubility. J. Nat. Prod. 81 (2018) 524-533.

[31]. C.P. Sun, C.Y. Qiu, F. Zhao, N. Kang, L.X. Chen, F. Qiu, Physalins V-IX, 16,24-cyclo-13, 14-seco withanolides from Physalis angulata and their antiproliferative and anti-inflammatory activities. Sci. Rep. 7 (2017).

Highlights

- Twenty nine novel ocotillol-type amide derivatives were designed and synthesized.
- The structure-activity relationship of the reversal activity was described.
- One novel derivative **6c** showed great reversal potency both *in vitro* and *in vivo*.
- The mechanism of the most potent compound **6c** acting on Pgp was first proved.